

# Microsomal triglyceride transfer protein regulates intracellular lipolysis in adipocytes independent of its lipid transfer activity

Sujith Rajan<sup>a</sup>, Peter Hofer<sup>b</sup>, Amanda Christiano<sup>a</sup>, Matthew Stevenson<sup>a</sup>, Louis Ragolia<sup>a</sup>,  
Eugenia Villa-Cuesta<sup>c</sup>, Susan K. Fried<sup>d</sup>, Raymond Lau<sup>e</sup>, Collin Braithwaite<sup>e</sup>,  
Rudolf Zechner<sup>b,g,h</sup>, Gary J. Schwartz<sup>f,\*</sup>, M. Mahmood Hussain<sup>a,i,\*\*</sup>

<sup>a</sup> Department of Foundations of Medicine, New York University Long Island School of Medicine, Mineola, NY 11501, United States of America

<sup>b</sup> Institute of Molecular Biosciences, University of Graz, Graz, Austria

<sup>c</sup> Department of Biology, College of Arts and Science, Adelphi University, Garden City, NY 11530, United States of America

<sup>d</sup> Diabetes, Obesity, and Metabolism Institute, Icahn School of Medicine at Mount Sinai, New York, NY, United States of America

<sup>e</sup> Department of Surgery, New York University Long Island School of Medicine, Mineola, NY 11501, United States of America

<sup>f</sup> Department of Medicine and Neuroscience, Albert Einstein College of Medicine, Bronx, NY 10461, United States of America

<sup>g</sup> BioTechMed-Graz, Austria

<sup>h</sup> BioHealth Field of Excellence, University of Graz, Graz, Austria

<sup>i</sup> Veterans Affairs New York Harbor Healthcare System, Brooklyn, NY, United States of America

## ARTICLE INFO

### Keywords:

Thermogenesis  
Free fatty acids  
Protein-protein interactions  
Obesity  
ATGL  
HSL

## ABSTRACT

**Background:** The triglyceride (TG) transfer activity of microsomal triglyceride transfer protein (MTP) is essential for lipoprotein assembly in the liver and intestine; however, its function in adipose tissue, which does not assemble lipoproteins, is unknown. Here we have elucidated the function of MTP in adipocytes.

**Approach and results:** We demonstrated that MTP is present on lipid droplets in human adipocytes. Adipose-specific MTP deficient (*A-Mtp*<sup>-/-</sup>) male and female mice fed an obesogenic diet gained less weight than *Mtp*<sup>f/f</sup> mice, had less fat mass, smaller adipocytes and were insulin sensitive. *A-Mtp*<sup>-/-</sup> mice showed higher energy expenditure than *Mtp*<sup>f/f</sup> mice. During a cold challenge, *A-Mtp*<sup>-/-</sup> mice maintained higher body temperature by mobilizing more fatty acids. Biochemical studies indicated that MTP deficiency de-repressed adipose triglyceride lipase (ATGL) activity and increased TG lipolysis. Both wild type MTP and mutant MTP deficient in TG transfer activity interacted with and inhibited ATGL activity. Thus, the TG transfer activity of MTP is not required for ATGL inhibition. C-terminally truncated ATGL that retains its lipase activity interacted less efficiently than full-length ATGL.

**Conclusion:** Our findings demonstrate that adipose-specific MTP deficiency increases ATGL-mediated TG lipolysis and enhances energy expenditure, thereby resisting diet-induced obesity. We speculate that the regulatory function of MTP involving protein-protein interactions might have evolved before the acquisition of TG transfer activity in vertebrates. Adipose-specific inhibition of MTP-ATGL interactions may ameliorate obesity while avoiding the adverse effects associated with inhibition of the lipid transfer activity of MTP.

**Abbreviations:** ApoB-Lps, apoB-containing lipoproteins; ATGL, adipose triglyceride lipase activity; ATGLi, ATGL inhibitor; CLAMS, comprehensive laboratory animal monitoring system; CGI-58, comparative gene identification-58; DEXA, dual-energy X-ray absorptiometry; FFA, free fatty acid; HSL, hormone sensitive lipase; HSLi, HSL inhibitor; LD, lipid droplet; MTP, microsomal triglyceride transfer protein; NBD, nitrobenzoxadiazole; OCR, oxygen consumption rate; RER, respiratory exchange ratio; SVF, stromal vascular fraction; TG, triglyceride.

\* Corresponding author.

\*\* Correspondence to: M. Hussain, Department of Foundations of Medicine, New York University Long Island School of Medicine, Mineola, NY 11501, United States of America.

E-mail addresses: [gary.schwartz@einsteinmed.edu](mailto:gary.schwartz@einsteinmed.edu) (G.J. Schwartz), [Mahmood.hussain@nyulangone.org](mailto:Mahmood.hussain@nyulangone.org) (M.M. Hussain).

<https://doi.org/10.1016/j.metabol.2022.155331>

Received 12 July 2022; Accepted 6 October 2022

Available online 10 October 2022

0026-0495/© 2022 Elsevier Inc. All rights reserved.

## 1. Introduction

Microsomal triglyceride (TG) transfer protein (MTP) resides in the endoplasmic reticulum and Golgi bodies, where it transfers lipids, and is essential for the synthesis and secretion of apoB-containing lipoproteins (apoB-Lps) in enterocytes and hepatocytes [1,2]. Lipid transfer activity inhibitors of MTP decrease plasma lipid levels and are used to treat hypercholesterolemia [3,4]. However, these treatments are associated with hepatosteatosis [5]. Loss of function mutations in the *MTTP* gene in people with abetalipoproteinemia are associated with an absence of apoB-Lps in the plasma [2,6]. Beyond hepatocytes and enterocytes, antigen presenting cells [7] that do not express apoB also express MTP. MTP interacts with apoB [8–10] and CD1 proteins [11,12]. In both cases, these proteins are loaded with lipids: several hundred-lipid molecules are added to assemble an apoB-Lp particle [1], whereas one phospholipid molecule is added to nascent CD1 proteins [12]. Thus, the lipid transfer activity of MTP is a unique, functionally important feature of this protein.

MTP has been shown to be present on lipid droplets (LDs) in 3T3-L1 cells [13,14]. MTP expression increases during adipogenesis, but MTP inhibition has no effect on 3T3-L1 pre-adipocyte differentiation [13]. In our previous study, we showed that MTP activity increases during differentiation of 3T3-L1 cells [15]. To define the role of adipose MTP, we crossed *Mtp<sup>f/f</sup>* mice with *Ap2<sup>Cre</sup>* mice and generated adipocyte- and macrophage-specific MTP deficient (*A,M-Mtp<sup>-/-</sup>*) mice. On an obesogenic (60 % kcal fat) diet, both male and female *A,M-Mtp<sup>-/-</sup>* mice had smaller adipocytes and gained significantly less weight than *Mtp<sup>f/f</sup>* mice, despite consuming similar amounts of food [15]. Swift et al. reported that *A,M-Mtp<sup>-/-</sup>* (*Ap2<sup>Cre</sup>*) and *A-Mtp<sup>-/-</sup>* (*Adipoq<sup>Cre</sup>*) mice fed a different high fat diet (43 % kcal fat), had smaller adipocytes in the gonadal and brown adipose tissue, yet gained similar amounts of weight to *Mtp<sup>f/f</sup>* mice [16]. These two studies using two different diets show a common phenotype of smaller adipocyte size in MTP deficient mice. However, both studies did not explain the mechanisms for the smaller adipocytes; hence, MTP's function in adipocytes remains unknown. In the current study, we show that adipose MTP plays a novel role in fat storage and mobilization by interacting and inhibiting lipolysis by adipose triglyceride lipase (ATGL) via a mechanism that does not require the lipid transfer activity of MTP. We speculate that the inhibition of MTP-ATGL interactions might be useful in the treatment of obesity.

## 2. Materials and methods

### 2.1. Animals

C57BL/6 (catalog # 000664) and B6.FVB-Tg(*Adipoq-cre*)1Evdr/j (catalog # 028020) mice were purchased from The Jackson Laboratory. B6.FVB-Tg(*Adipoq-cre*)1Evdr/j mice were backcrossed more than seven times with C57BL/6 mice. These *Adipoq-cre* mice were crossed with *Mtp<sup>f/f</sup>* mice on C57BL/6 background to get adipose-specific MTP knockout mice (*A-Mtp<sup>-/-</sup>*). *Mtp<sup>f/f</sup>* and *A-Mtp<sup>-/-</sup>* mice were bred separately at the NYU Long Island School of Medicine (NYU LISOM) vivarium at a temperature of 21–23 °C under a normal 12 h light/dark cycle. They were fed a chow diet (catalog #5053, PicoLAB Rodent Diet 20, LabDiet) containing calories from fat (13 %), protein (25 %) and carbohydrates (62 %). At 8 to 12 weeks of age, mice were switched to an obesogenic diet (D12492, Research Diets Inc., New Brunswick, NJ) deriving calories from fat (60 %), protein (20 %), and carbohydrate (20 %) for the duration of the study. In some experiments, these mice received a Western diet (TD.88137, Envigo) containing 43 % fat, 15 % protein and 43 % carbohydrate calories. NYU LISOM's Institutional Animal Use and Care Committee, which adheres to guidelines provided by the National Institutes of Health, approved all experiments and animal care protocols.

### 2.2. Body composition and metabolic phenotype assessment

Mice were anesthetized and body mass composition was analyzed using Faxitron Micro Focus Imaging System-UltraFocus100. Locomotor activity, oxygen consumption and carbon dioxide production were monitored with Comprehensive Lab Animal Monitoring System (Oxy-max®-CLAMS, Columbus Instruments, Columbus, OH). Data from the first 24 h were excluded from analyses, as this period allowed mice to acclimatize and familiarize with single housing and drinking in the cages. Data were separated based on light–dark cycle and are presented as means  $\pm$  SD.

### 2.3. Thermoneutral and cold challenge experiments

After 4 months on an obesogenic diet at NYU LISOM, *Mtp<sup>f/f</sup>* and *A-Mtp<sup>-/-</sup>* mice were shipped to the Albert Einstein College of Medicine and acclimatized for 2 weeks on the same obesogenic diet at room temperature. These mice were then transferred to rooms maintained at 30 °C with *ad libitum* access to the same obesogenic diet. The body weight and body composition were monitored weekly. The mice metabolic phenotype was monitored at 30 °C as mentioned before. Mice were implanted with telemetry devices (TA-F10, Data Sciences International) to measure core body temperature and metabolic phenotype was analyzed in CLAMS at cold (6 °C) temperature for 2 h. Blood was collected at the end of the cold challenge to measure plasma FFA level.

### 2.4. $\beta$ 3-Adrenergic receptor stimulation

Male *Mtp<sup>f/f</sup>* and *A-Mtp<sup>-/-</sup>* mice fed an obesogenic diet were fasted overnight, and blood was collected before stimulation with CL316243 (1 mg/kg body weight) via IP injection. Fifteen minutes later, blood was again collected from retro-orbital vein. Plasma was used to measure FFA levels.

### 2.5. Glucose homeostasis

Intraperitoneal glucose tolerance (IPGTT) and insulin tolerance (ITT) tests were performed as reported earlier [17,18]. Fasting insulin levels were measured using insulin ELISA kit from Crystal Chem (Catalog No: #90080) according to the manufacturer's instructions. Homeostatic model for assessment of insulin resistance (HOMA-IR) was calculated using fasting glucose and insulin level.  $\text{HOMA-IR} = \text{fasting glucose (mg/dL)} \times \text{fasting insulin (mg/dL)} / 405$ .

### 2.6. Expression of enzymes in Cos-7 cells

Cos-7 cells (3 million) were seeded in 150 mm dishes and cultured in DMEM containing 10 % FBS and 1 % antibiotic solution. After 24 h, cells received Opti-MEM medium and were transfected with 30  $\mu$ g of pcDNA3 (control plasmid) or plasmid expressing human ATGL [19], mouse HSL [19], CGI-58 (OriGene, catalog # RC201869), or mouse ATGL [19] using EndoFectin (2.5  $\mu$ L per  $\mu$ g of plasmid). After 24 h of transfection, cells were trypsinized and reverse transfected with 7.5  $\mu$ g of either pcDNA3, human wild type MTP or N780Y mutant MTP. After 14–16 h of transfection, the medium was changed to DMEM containing 10 % FBS without antibiotics. After 48 h, cells were washed with ice cold PBS and harvested in 1 mL of buffer K (1 mM Tris-HCl, pH 7.6, 1 mM EGTA, and 1 mM MgCl<sub>2</sub>) containing 10  $\mu$ L/mL of protease inhibitor cocktail (catalog # P2714, Sigma) in preparation for homogenization.

### 2.7. Lipase assay using NBD-TAG vesicles

Nitrobenzoxadiazole-labeled TAG [(NBD-TAG; 1,3-di(cis-9-octadecenoyl)-2-((6-(7-nitrobenz-2-oxa-1,3-diazol-4-yl)amino)hexanoyl)glycerol)] vesicles were prepared as described previously [20]. Briefly, NBD-TAG (catalog # 6285) (1262.8 nmol), egg phosphatidylcholine (PC,

catalog # 131601, 176 nmol), and phosphatidylinositol (PI, catalog # P0639, 59 nmol) were added to 15 mM Tris, pH 7.4, 0.02 % sodium azide, 1 mM EDTA, 40 mM NaCl and sonicated (Sonic Dismembrator 550 from Fisher Scientific) on ice for 30 min until the mixture was clear. The clear solution was subjected to ultracentrifugation at 233,800g (50,000 rpm, SW50.1 Ti rotor) for 1 h at 10 °C. The top 4 mL of NBD-TAG vesicles were collected, 200 mg BSA and 650 mg NaCl was added, and the vesicles were stored at 4 °C until use. Lipase assays were performed in triplicate in opaque round bottom 96 well assay plate (catalog # 3792, Costar). The plate also contained a series of NBD-C6 dilutions representing a standard curve ranging from 0 to 1250 pmol as described previously [20]. To measure background fluorescence, NBD-TAG vesicles (10  $\mu$ L, 3155 pmol of NBD-TAG) were incubated at 37 °C with 100  $\mu$ L of buffer K without any enzyme source and NBD fluorescence was measured at 37 °C at different time points or at the end of 1 h incubation. To measure lipase activity, cell lysates were incubated with NBD-TAG vesicles in parallel. The blank fluorescence values were subtracted. Fluorescence was measured using excitation 460 nm and emission 530 nm wavelengths in Perkin Elmer Inspire multi plate reader.

In studies using expression of ATGL and MTP, the FFA were extracted after 1 h incubation with NBD-TAG vesicles by adding 3.25 mL of methanol/chloroform/heptane (10/9/7; vol/vol/vol) and 1 mL of 0.1 M potassium-carbonate/0.1 M boric acid (pH 10.5). The mixture was extensively vortexed and centrifuged at 800g for 10 min. Upper aqueous phase was collected and NBD fluorescence was measured using excitation 460 nm and emission 530 nm wavelengths in Perkin Elmer Inspire multi plate reader.

## 2.8. TG hydrolase activity using $^3$ H-triolein

TG substrate was prepared by emulsifying 330  $\mu$ M triolein (40,000 cpm nmol<sup>-1</sup> glycerol tri[9,10(n)- $^3$ H]-oleate (PerkinElmer)) and 45  $\mu$ M phosphatidylcholine/phosphatidylinositol (3:1) in 100 mM potassium phosphate buffer (pH 7.0) by sonication and adjusted to 5 % essentially FA-free BSA (Sigma, St Louis, MO) [21]. Purified proteins were incubated with 100  $\mu$ L of TG-substrate in a water bath at 37 °C for 60 min. As a control, incubations under identical conditions were performed using flag peptide alone. After incubation, the reaction was terminated by adding 3.25 mL of methanol/chloroform/heptane (10/9/7; vol/vol/vol) and 1 mL of 0.1 M potassium-carbonate/0.1 M boric acid (pH 10.5). The mixture was vortexed and centrifuged at 800g for 10 min, 200  $\mu$ L of upper aqueous phase was collected and the radioactivity was measured by liquid scintillation counting (Tri-Carb 2100TR).

## 2.9. Human SVF isolation and differentiation into adipocytes

The stromal vascular fraction (SVF) was isolated from subcutaneous adipose tissue obtained from 4 patients (Supplementary Table 1) undergoing bariatric surgery and other surgeries at NYU LISOM (IRB protocol #1127649), using collagenase digestion as described previously [18,22]. Briefly, subcutaneous adipose tissues were minced and washed thoroughly in phosphate buffer saline (PBS) containing 1 % penicillin/streptomycin solution. Washed samples were digested with 1 % collagenase Type-I for 30 min at 37 °C. Dulbecco's modified Eagle's medium (DMEM) containing 20 % fetal bovine serum (FBS) was added to inhibit the collagenase activity and centrifuged at 400g for 10 min. The cell pellet was suspended in DMEM and filtered through a 70  $\mu$ M cell strainer. The resultant SVF suspension was seeded in a T75 flask containing DMEM with 10 % FBS. Human SVF (hSVF) was cultured in high-glucose DMEM supplemented with 10 % fetal bovine serum and antibiotics. hSVF was seeded in 6 well plates at density of 200,000 cells per well and grown till confluent. hSVF was differentiated into adipocytes using a differentiation cocktail containing 500  $\mu$ M IBMX, 5  $\mu$ g/ml insulin, 1  $\mu$ M dexamethasone, 200  $\mu$ M indomethacin and 1  $\mu$ M of rosiglitazone. Cells were maintained in differentiation cocktail containing

medium for 3 days. Differentiation medium was replaced with media containing 5  $\mu$ g/mL insulin and maintained for additional 2 days. The differentiated adipocytes were maintained in DMEM for 1 day and were used for different experiments.

## 2.10. Isolation of mouse SVF

Inguinal adipose tissue from male *Mtp*<sup>f/f</sup> and *A-Mtp*<sup>-/-</sup> mice (n = 3) fed an obesogenic diet for 6-months were collected in PBS and minced. The minced tissue was incubated with digestion buffer (1.5 U/mL of collagenase D, 2.4 U/mL of dispase II and 10 mM CaCl<sub>2</sub>) for 30 min to 1 h until the tissue and digestion buffer become homogeneous. The digestion was stopped by adding an equal volume of 0.5 % BSA and centrifuged at 300g for 5 min at room temperature. The cell pellet was re-suspended in 0.5 % BSA and passed through a 100  $\mu$ M cell strainer. The flow through was centrifuged again at 300g for 5 min at room temperature and the pellet was re-suspended in 0.5 % BSA and passed through 40  $\mu$ M cell strainer. The flow through was centrifuged at 300g for 5 min and resultant pellet was re-suspended in DMEM containing 10 % FBS supplement with 1 % antibiotics (penicillin and streptomycin) and transferred to a T75 flask. The media was changed the next day. Mouse SVF was differentiated similarly to human SVF as described above. Mouse SVF was differentiated to brown adipocytes as before [17,18] using triiodothyronine (T3, 10 nM) along the differentiation cocktail.

## 2.11. Gene expression analysis using qRT-PCR

Total RNA was isolated from different organs using TRIZOL reagent. RNA concentrations were measured using Nano Drop (Thermo Scientific™, USA, #ND-2000). Total RNA (2000 ng) was used to synthesize first strand cDNA using Applied Biosystems™ High-Capacity cDNA Reverse Transcription Kit (Thermo Scientific™, USA, #4368813). Synthesized cDNA was then used for quantitative real-time PCR analysis on ABI Prism 7000HT Sequence Detection System (Applied Biosystem) using the SYBR green master mix (Applied Biosystems, Thermo Fisher Scientific, Cambridge, MA). The expression of candidate genes was normalized to endogenous 18S RNA. The analysis of quantitative real time PCR was obtained by using ( $2^{-\Delta\Delta Ct}$ ) method.

## 2.12. Histological analyses

Epididymal (eWAT) and inguinal (iWAT) white adipose tissue and interscapular brown adipose tissue (iBAT) were excised and fixed in 4 % paraformaldehyde. Fixed tissue was embedded in paraffin and cut in 8  $\mu$ m thick sections. All sections were deparaffinized and stained with hematoxylin and eosin (H&E) and imaged using a Nikon A1 confocal microscope (Melville, NY) at 10 $\times$  magnification. Adipocyte sizes (eWAT, iWAT) were measured using Fiji imaging software with the Adiposoft v1.16 plugin with both automated and manual input. A total of 287 (*Mtp*<sup>f/f</sup>) and 341 (*A-Mtp*<sup>-/-</sup>) eWAT and 419 (*Mtp*<sup>f/f</sup>) and 491 (*A-Mtp*<sup>-/-</sup>) iWAT adipocyte areas were measured for adipocyte size distribution plots.

## 2.13. Oil red O staining

Oil red O staining was performed as previously described [23]. Adipocyte lipid droplets were stained with Oil red O (0.36 % in 60 % isopropanol) for 20 min, washed with PBS three times and photographed. In addition, accumulated dye was extracted using 100 % isopropanol, and absorbance was measured at 490 nm.

## 2.14. Immunoprecipitation of CGI-58 and MTP from human adipocytes

Adipocytes differentiated from human SVF were lysed and 400  $\mu$ g protein was taken for immunoprecipitation. A small amount (25  $\mu$ g) was

used to check the expression of ATGL and  $\beta$ -Actin. The cell lysates were first incubated with host IgG of CGI-58 and MTP along with 40  $\mu$ L of A/G agarose beads (Catalog no: # sc2003, Santa Cruz Biotech) for 1 h at 4 °C to limit non-specific interactions. The samples were centrifuged at 100g for 5 min and the supernatants were collected. The supernatants were incubated overnight with either mouse IgG, rabbit IgG (negative control), CGI-58 (positive control) or MTP antibody and gently rotated overnight in a rotator at 4 °C. A/G agarose beads (40  $\mu$ L) were incubated with 5 % milk to block non-specific binding and transferred to cell lysates incubated with antibody. The cell lysates were further incubated for 1 h with antibody and A/G beads in a rotator at 4 °C and centrifuged at 100g for 5 min. The beads were pelleted and washed 3 times with PBS containing 0.1 % Tween 20. Laemmli sample buffer (2 $\times$ ) with  $\beta$ -mercaptoethanol was added to the washed beads, boiled for 10 min, centrifuged at 1000g for 2 min and the supernatants were loaded for SDS-PAGE. Proteins were transferred to nitrocellulose membranes, blocked with 5 % milk, incubated with primary antibodies. Veriblot (1:2000, Abcam, ab131366) in 2 % BSA was used as secondary antibody for the detection of different proteins.

#### 2.15. Co-immunoprecipitation of proteins expressed in HEK293T cells

HEK-293T cells (ATCC CRL-3216) were maintained in DMEM High Glucose (Thermo Scientific, USA, #41966052) and transfected using Metafectene (Biontex, Germany, #T020) according to the manufacturer's instructions. The coding sequences of human and mouse ATGL were expressed from the pcDNA4/HisMax vector (Invitrogen, USA) [19]. In case of ATGL288\*, a premature stop codon was introduced after the triplet encoding for D288 in the mouse ATGL construct using the Q5® Site-Directed Mutagenesis Kit (New England BioLabs, USA, #E0554S) [24]. Twenty-four hours after transfection, cells were lysed and co-immunoprecipitation was performed as described previously [24]. Anti-Xpress antibody (Thermo Fisher Scientific #R910-25) was used to detect Xpress-Tagged proteins.

#### 2.16. Western blot analysis

Protein lysates were denatured by heating at 65 °C for 10 min in Laemmli sample buffer supplemented with 10 %  $\beta$ -mercaptoethanol and protein was resolved by 8 to 12 % SDS-PAGE and transferred onto nitrocellulose membranes using an Amersham Transblot apparatus (at 50 V for 3 h). Membranes were blocked for 2 h at room temperature in 5 % skim milk (Sigma) in Tris-buffered saline (TBS; 10 mM Tris pH 7.6, 150 mM NaCl) containing 0.05 % Tween-20 (TBS-T). After washing with TBS-T, membranes were incubated with target protein specific antibodies (2 % BSA in TBS, 1:1000 dilution) overnight at 4 °C, followed by incubation with appropriate HRP-conjugated secondary antibodies (2 % BSA in TBS, 1:5000 dilution) for 1 h. The target proteins were detected using an Immobiline western Chemiluminescence detector (Millipore; Billerica, USA) on a BioRad Image-Doc Touch imaging system. To validate equal loading in each lane,  $\beta$ -actin was used as an internal loading control. Quantitation of protein levels was performed using Image J software (NIH).

#### 2.17. Oxygen consumption rate (OCR) studies in adipocytes

OCR was measured as described previously [17]. Mouse and human SVF were differentiated in 6 well plates. Cells were detached using 1 $\times$  trypsin containing 0.5 % collagenase type 1A. DMEM media containing 10 % FBS was added to the cells to neutralize trypsin and collagenase type 1A. Cells were collected and centrifuged at 300g for 5 min at room temperature. Resulting adipocyte pellets were resuspended in culture media and seeded in 24 well xFe extracellular flux analyzer culture plates. After 16 h, DMEM was replaced with assay medium (Agilent Technologies, Inc., catalog # 103575-100) and incubated for 2 h at 37 °C in a non CO<sub>2</sub> incubator. We used 1  $\mu$ M oligomycin, 1  $\mu$ M FCCP and

0.5  $\mu$ M rotenone/antimycin A mixture as per manufacturer's protocol (Agilent Technologies, Inc., catalog #103015-100). Readings were normalized to total protein concentration.

#### 2.18. Immunostaining

Adipocytes were plated in 8 chambered polystyrene vessel tissue culture treated glass slides. After 16 h, adipocytes were washed twice with PBS, fixed with 4 % paraformaldehyde for 10 min at room temperature, rinsed with PBS thrice, permeabilized by incubating with 0.3 % Triton X-100 containing PBS for 5 min, rinsed thrice with PBS, blocked with 5 % goat serum in PBS for 1 h, and probed with primary antibody (anti-MTP 1:200 dilution, anti-ATGL 1:250 dilution or anti-CGI 58 1:250 dilution) for 2 h in 5 % goat serum containing PBS at room temperature. For controls, similar dilutions of mouse rabbit and goat IgG isotypes (1 mg/mL) were used. Adipocytes were washed and probed with secondary antibody conjugated with different fluorophores for 1 h in 5 % goat serum containing PBS at room temperature, washed thrice with PBS. The bottom slide of 8 chambered slide was detached and mounted on a glass slide coated with prolonged gold antifade reagent with DAPI. Slides were visualized using a Nikon ECLIPSE Ti confocal microscope at 40 $\times$  and 100 $\times$  using oil immersion lenses.

#### 2.19. Triglyceride transfer assay

Cell lysates (35  $\mu$ g) prepared in buffer K containing protease inhibitor cocktail were incubated with donor vesicles containing NBD-labeled triolein (Catalog # 6285, Setareh Biotech) and acceptor vesicles [25,26]. Fluorescence was measured at different time intervals (5, 10, 15, 30, 45 and 60 min) using fluorimeter (Perkin Elmer Enspire). Percent triglyceride transfer was calculated after subtracting the blank and dividing it by the total fluorescence reading obtained by disrupting vesicles with isopropanol as previously described [25,26].

#### 2.20. Purification of Flag-tagged proteins using anti-Flag M2 affinity column

Cos-7 cells were transfected with 30  $\mu$ g of pcDNA3.1 expression plasmids encoding different Flag-tagged wild type MTP, mutant MTP, and CGI58 proteins. After 48 h of transfection, cells were washed three times with ice cold PBS and scraped in buffer K (1 mM Tris-HCL, 1 mM EGTA and 1 mM MgCl<sub>2</sub>, pH 7.6) containing protease inhibitor cocktail (Sigma, catalog # P2714). Cells were mechanically lysed by passing 10 times through a 30 $\frac{1}{2}$  gauge needle, and small fractions were used to measure the total protein using a BCA protein assay (catalog #b1856209, Thermo Scientific). Cell lysates were incubated overnight with anti-Flag M2 affinity Gel (Sigma, catalog # A2220). The bound Flag-tagged protein were washed and eluted using 100  $\mu$ M FLAG peptide (Genscript) in 2 mL PBS. The eluted fractions were added on top of 3 K Amicon Ultra-15 centrifugal filters and centrifuged at 3000 rpm for 1 h. Purified Flag-tagged proteins (5  $\mu$ L) were run on 8 % SDS-PAGE gel. The separated proteins were transferred to nitrocellulose membranes and probed with anti-Flag M2 (1:1000 dilution, catalog # F3165, Sigma-Aldrich) prepared in TBS containing 2 % BSA. The blots were washed and probed with HRP-conjugated appropriate secondary antibodies (Anti-rabbit 1:5000 dilution, catalog #7074, Cell Signaling Technology, Anti-mouse 1:5000 dilution, catalog # 62-6520, Invitrogen). The blots were developed in ChemiDoc™-Touch Imaging system from Bio Rad.

#### 2.21. ELISA based protein-protein interaction studies

High binding ELISA plates were coated with purified Flag-tagged wild-MTP, N780Y mutant MTP, or CGI58 proteins and incubated overnight. The wells were washed thrice with washing buffer (PBS containing 0.05 % tween-20), blocked with 5 % BSA in buffer K, washed, and incubated with 50  $\mu$ g of protein/well of Cos-7 cells extracts

containing His-Tagged proteins in Buffer K for 3 h. Wells were washed thrice with washing buffer, probed with mouse anti-His antibody (1:1000 dilution) in 2 % BSA in Buffer K for 1 h, washed thrice, probed with HRP conjugates anti-mouse antibody (1:5000 dilution), and incubated for 1 h and developed by adding 100  $\mu$ L of tetramethylbenzidine (Thermo Scientific, catalog # 1854060, 1,854,050). Absorbance was measured at 450 nm (PerkinElmer Enspire multi plate reader) after adding 50  $\mu$ L of stop solution.

## 2.22. MTT assay for cell viability and proliferation

MTT assay was done as described previously [17]. Briefly, SVF from *Mtpp<sup>f/f</sup>* and *A-Mtpp<sup>-/-</sup>* mice were plated in 96-well plates at a density of 10,000 cells per well. The plates were maintained in growth medium at 37 °C. At 24 h and 48 h MTT assay was performed by replacing the media with 300  $\mu$ L of MTT reagent (0.015 g of MTT reagent dissolved in 30 mL of media). Plates were incubated for 3 h at 37 °C and 200  $\mu$ L of DMSO was added to each aspirated wells. Absorbance was taken at 540 nm.

## 2.23. Statistical analysis

Data analysis was performed using Prism software (Version 9, GraphPad Software). Results were expressed as mean  $\pm$  standard deviation (SD). Statistical significance was determined using a two-tail Student's *t*-test when the experiment contained two groups, or one-way ANOVA was performed when comparing more than two groups. Two way repeated measures ANOVA was performed in experiments where time was included as a second parameter, statistical significance was set at *p* < 0.05. The *p* value for statistical significance of each test is reported in each figure legend.

## 3. Results

### 3.1. MTP is on LDs in human adipocytes

To determine whether MTP is present on LDs in human adipocytes, we isolated the stromal vascular fraction (SVF) from human subcutaneous fat, differentiated into adipocytes, and quantified MTP and apoB mRNA levels. The apoB mRNA levels in human adipocytes were very low (Ct value > 31), whereas the levels were readily quantifiable in human hepatoma Huh-7 cells (Supplementary Fig. 1A). Comparative analysis demonstrated ~2000-fold fewer apoB mRNA in adipocytes than in Huh-7 cells. In contrast, MTP mRNA levels were detectable in human adipocytes and were ~100-fold fewer than those in hepatoma cells (Supplementary Fig. 1B). We then assessed whether human MTP is on LDs. MTP co-localized with Lipitox-stained LDs similarly to another LD protein, CGI-58 (Fig. 1A). Furthermore, MTP co-localized with the LD proteins CGI-58 and ATGL (Fig. 1B). These results indicate that MTP is expressed in human adipocytes and is present on LDs.

### 3.2. *A-Mtpp<sup>-/-</sup>* mice fed an obesogenic diet show elevated energy expenditure and diminished weight gain

To uncover MTP's function in adipocytes, we generated adipose specific MTP knockout mice (*A-Mtpp<sup>-/-</sup>*) by crossing *Mtpp<sup>f/f</sup>* mice with *AdipoQ<sup>Cre</sup>* mice (Supplementary Fig. 2A). We observed no significant differences in body composition and metabolic parameters when male (Supplementary Fig. 2B–N) and female (Supplementary Fig. 3A–M) *A-Mtpp<sup>-/-</sup>* mice were fed a chow (13 % kcal fat) diet for 6 months. Male *A-Mtpp<sup>-/-</sup>* mice on a 43 % kcal fat diet gained weight similarly to *Mtpp<sup>f/f</sup>* mice (Supplementary Fig. 4A). Body composition analysis and metabolic studies revealed no significant differences between *A-Mtpp<sup>-/-</sup>* and *Mtpp<sup>f/f</sup>* mice (Supplementary Fig. 4B–N). Similarly, female *A-Mtpp<sup>-/-</sup>* mice on a 43 % kcal fat diet did not show any difference in weight gain and metabolic activity compared with *Mtpp<sup>f/f</sup>* mice (Supplementary Fig. 4O–S), in agreement with a study conducted by Swift et al. [16].

In contrast when fed an obesogenic diet (60 % kcal fat), both male

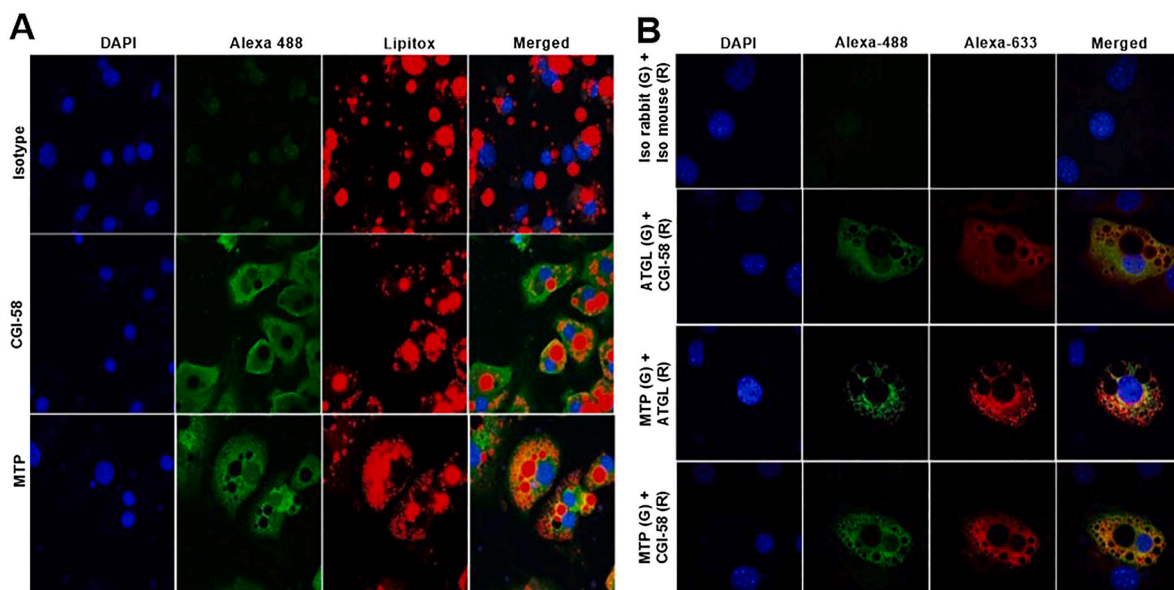


**Fig. 1.** MTP is on LDs in human adipocytes.

(A) Adipocytes differentiated from human SVF were stained with DAPI (blue), Lipitox (red, lipid droplets), and anti-CGI-58 or anti-MTP antibodies (green). Mouse and rabbit IgG were used as isotype controls. Images were taken at 40 $\times$  magnification. Co-localization of proteins with lipid droplets is indicated by yellow in the merged images.

(B) Adipocytes differentiated from human SVF were stained with DAPI (blue), anti-MTP (green), anti-CGI-58 (CGI, red) or anti-ATGL (green or red) antibodies. Mouse and rabbit IgG were used as isotype controls. Images were taken at 100 $\times$  magnification with a Nikon Ti Eclipse confocal microscope. The yellow color shows co-localization of proteins on merged images. (For interpretation of the references to color in this figure legend, the reader is referred to the web version of this article.)

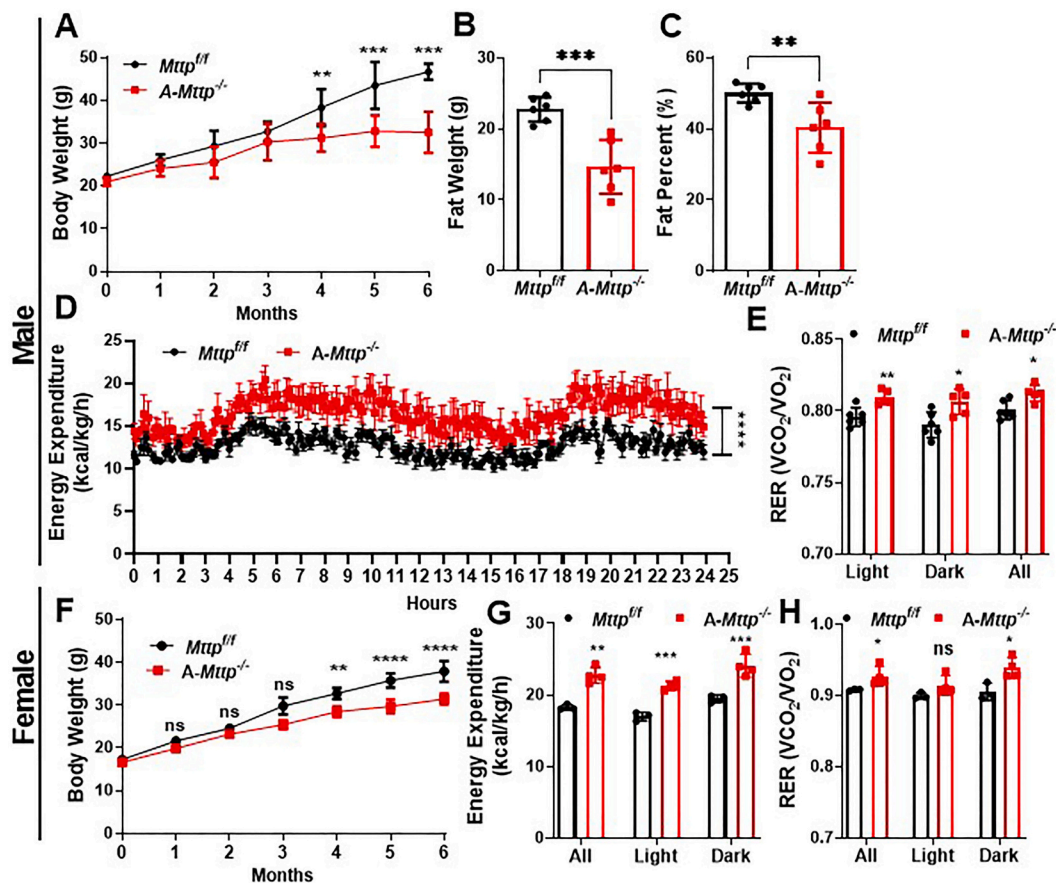


**Fig. 2.** *A-Mtp<sup>-/-</sup>* mice fed an obesogenic diet show elevated energy expenditure and diminished weight gain.

Male *Mtp<sup>f/f</sup>* and *A-Mtp<sup>-/-</sup>* mice (12 weeks old,  $n = 6$  per group) were fed *ad libitum* an obesogenic diet and maintained at 23 °C. (A) Body weight was measured monthly.

(B–C) In a separate experiment, *Mtp<sup>f/f</sup>* and *A-Mtp<sup>-/-</sup>* mice ( $n = 6$ ) were fed an obesogenic diet for 5 months and subjected to DEXA analysis at room temperature (23 °C) to determine (B) fat mass and (C) fat percentage.

(D–E) The same set of mice was used for metabolic studies in CLAMS at 23 °C to measure (D) energy expenditure and (E) RER.

(F) Female *Mtp<sup>f/f</sup>* and *A-Mtp<sup>-/-</sup>* mice (12-weeks-old) ( $n = 3–4$ ) were fed an obesogenic diet (60 % kcal fat) for 6 months, and body weight was monitored monthly.

(G–H) (G) Energy expenditure, (H) RER were measured in obesogenic diet fed female *Mtp<sup>f/f</sup>* and *A-Mtp<sup>-/-</sup>* mice ( $n = 3–4$ ).

Bars and error bars represent mean  $\pm$  SD. Significance was calculated with two-way ANOVA followed by multiple comparison for graph A and F. Ordinary two-way ANOVA repeated measure were used to calculate the significance for graph D. Student's *t*-test in B, C, E, G, and H. \* $P < 0.05$ , \*\* $P < 0.01$ , \*\*\* $P < 0.001$  and \*\*\*\* $P < 0.0001$ .

(Fig. 2A) and female (Fig. 2F) *A-Mtp<sup>-/-</sup>* mice gained significantly less weight than control mice, in agreement with studies in *A-Mtp<sup>-/-</sup>* mice [15]. These results indicated that *A-Mtp<sup>-/-</sup>* mice are resistant to weight gain on an obesogenic diet. To identify the biological bases underlying the lower weight gain, we analyzed body composition and metabolic parameters at 23 °C. DEXA analysis revealed significantly less fat mass, and fat percentage in male *A-Mtp<sup>-/-</sup>* mice than *Mtp<sup>f/f</sup>* mice (Fig. 2B, C), with no difference in lean mass, bone mineral density or bone mineral content (Supplementary Fig. 5A–C). Male *A-Mtp<sup>-/-</sup>* mice showed higher energy expenditure than *Mtp<sup>f/f</sup>* mice when normalized to body weight (Fig. 2D) or without normalizing with body weight (Supplementary Fig. 5D), and RER (Fig. 2E), but did not differ in food intake and locomotor activity levels (Supplementary Fig. 5D, E). These studies suggested that a reason for the lower weight gain in *A-Mtp<sup>-/-</sup>* mice might be less accretion of fat mass and higher energy expenditure.

Female *A-Mtp<sup>-/-</sup>* mice also gained less weight (Fig. 2F) and showed significantly greater energy expenditure and RER (Fig. 2G–H) than female *Mtp<sup>f/f</sup>* mice on an obesogenic diet. However, the food intake and locomotor activity were similar between female *A-Mtp<sup>-/-</sup>* and *Mtp<sup>f/f</sup>* mice (Supplementary Fig. 6A, B). Thus, male and female *A-Mtp<sup>-/-</sup>* mice respond similarly to an obesogenic diet and gain less fat mass, owing to higher energy expenditure.

### 3.3. *A-Mtp<sup>-/-</sup>* mice mobilize free fatty acids (FFA) to a greater extent than control mice under stress

Mice at 23 °C are under constant cold stress, and to maintain normal body temperature their basal metabolism is three times higher than that at thermoneutral conditions [27,28]. We hypothesized that *A-Mtp<sup>-/-</sup>* mice expended more energy because they were kept below their body temperatures. Consequently, we studied their energy expenditure at thermoneutral temperature (30 °C). Male mice were first fed an obesogenic diet at room temperature and transferred to rooms maintained at 30 °C, where they were then maintained on the same diet. The *A-Mtp<sup>-/-</sup>* mice slowly gained weight, and their weights normalized to those of *Mtp<sup>f/f</sup>* mice within 6 weeks (Fig. 3A). Similarly, the fat mass of *A-Mtp<sup>-/-</sup>* mice gradually increased and became similar to that of *Mtp<sup>f/f</sup>* mice (Fig. 3B). We also observed an increase in lean mass in *A-Mtp<sup>-/-</sup>* mice (Fig. 3C). Energy expenditure in both *Mtp<sup>f/f</sup>* and *A-Mtp<sup>-/-</sup>* mice at 30 °C (Fig. 3D) was lower than in mice at 23 °C (Fig. 2D). *A-Mtp<sup>-/-</sup>* mice showed significantly higher energy expenditure than *Mtp<sup>f/f</sup>* mice at 30 °C (Fig. 3D). We did not observe differences in RER and physical activity between *A-Mtp<sup>-/-</sup>* mice and *Mtp<sup>f/f</sup>* mice at 30 °C (Supplementary Fig. 7A, B). Overall, these results indicated that *Mtp<sup>f/f</sup>* mice maintain body weight, fat and lean mass over time at 30 °C, whereas *A-*

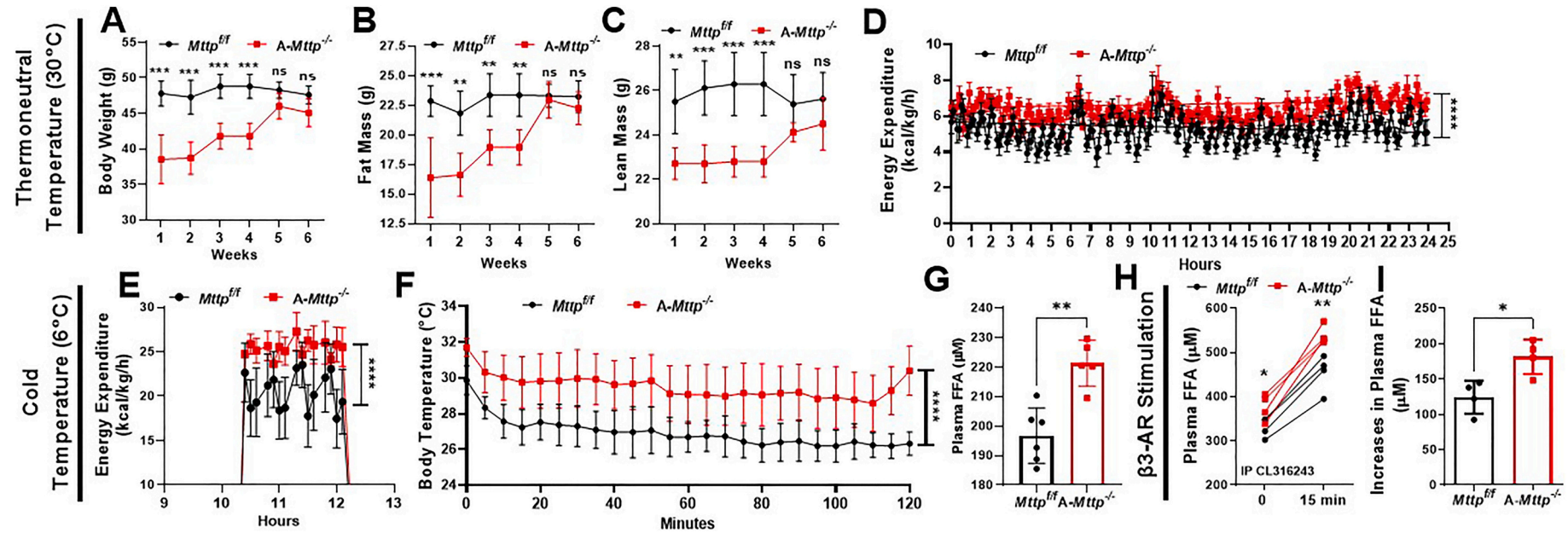


Fig. 3. *A-Mttp*<sup>-/-</sup> mice mobilize free fatty acids to a greater extent than control mice under stress.

(A–D) *Mttp*<sup>fl/fl</sup> and *A-Mttp*<sup>-/-</sup> mice ( $n = 4$ ) were fed an obesogenic diet for 4 months at NYU Long Island School of Medicine, then transferred to Albert Einstein College of Medicine. After acclimation, mice were transferred to a room maintained at 30 °C and continued on the same obesogenic diet for 6 weeks. Changes in (A) body weight, (B) fat mass, (C) lean mass were monitored weekly and (D) energy expenditure at the end of 6 week.

(E–G) The same set of mice was transferred to a room set at 6 °C for 2 h to study the effect of cold challenge, and their (E) energy expenditure and (F) body temperature were measured. (G) Plasma FFA concentrations were measured at the end.

(H–I) In another experiment, obesogenic diet fed *Mttp*<sup>fl/fl</sup> and *A-Mttp*<sup>-/-</sup> mice ( $n = 4$ ) were given IP injection of CL316243 (1 μg/kg) and blood was collected before and after injections. (H) Plasma FFA concentration before and 15 min after injection. (I) Increases in plasma FFA levels were calculated by subtraction of the initial plasma FFA concentration from 15-min values. Bars and error bars represent mean ± SD. Significance was calculated with two-way ANOVA followed by multiple comparison for graph A, B, C and H. Ordinary two-way ANOVA repeated measure were used to calculate the significance for graph D, E, and F. Student's *t*-test in G and I. \* $P < 0.05$ , \*\* $P < 0.01$ , \*\*\* $P < 0.001$  and \*\*\*\* $P < 0.0001$ .

*Mtp*<sup>-/-</sup> mice gain weight, fat mass and lean mass, eventually becoming indistinguishable from *Mtp*<sup>f/f</sup> mice. Thus, adipose MTP plays an important role in thermogenesis and under non-thermoneutral environmental stress conditions.

To further assess the importance of MTP in regulating fat metabolism under environmental stress, we subjected mice to a cold challenge (6 °C, 2 h). Both *Mtp*<sup>f/f</sup> and *A-Mtp*<sup>-/-</sup> mice demonstrated much higher energy expenditure at 6 °C (Fig. 3E) than at other temperatures (Figs. 3D and 2D). *A-Mtp*<sup>-/-</sup> mice showed higher energy expenditure (Fig. 3E) and maintained higher body temperature than *Mtp*<sup>f/f</sup> mice at 6 °C (Fig. 3F), whereas no differences were observed in RER and activity (Supplementary Fig. 7C, D). These studies indicated that *A-Mtp*<sup>-/-</sup> mice are

more efficient than *Mtp*<sup>f/f</sup> mice at maintaining a higher body temperature during a cold challenge. To fuel thermogenesis and maintain body temperature, mice mobilize FFA from WAT to the liver and brown adipose tissue (BAT) [29,30]. Therefore, we measured plasma FFA levels at the end of the cold challenge. *A-Mtp*<sup>-/-</sup> mice had significantly higher plasma FFA levels than *Mtp*<sup>f/f</sup> mice (Fig. 3G) indicating increased FFA mobilization. In summary, *A-Mtp*<sup>-/-</sup> mice mobilize more FFA and show higher energy expenditure.

Beyond cold challenge, acute stimulation of  $\beta_3$  adrenergic receptors also induces FFA mobilization from adipose tissue [31]. To test whether adrenergic stimuli might also increase FFA, we intraperitoneally administered CL316243 (1 mg/kg), a  $\beta_3$ -adrenergic agonist, to fasted A-

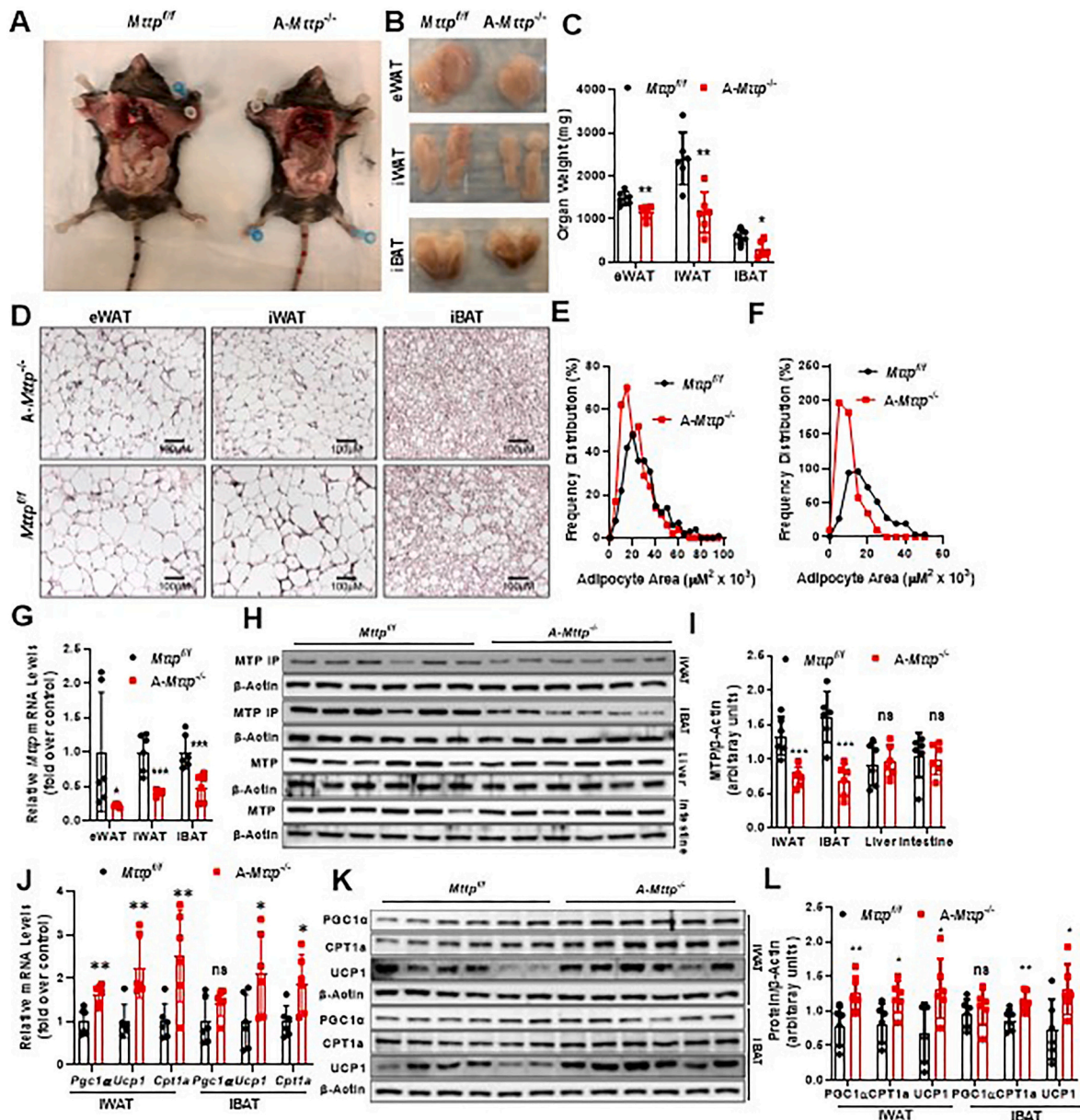


**Fig. 4.** *A-Mtp*<sup>-/-</sup> mice have smaller adipocytes than *Mtp*<sup>f/f</sup> mice and show elevated expression of thermogenic genes in iWAT and iBAT.

Male *Mtp*<sup>f/f</sup> and *A-Mtp*<sup>-/-</sup> mice were fed an obesogenic diet for 6 months. (A) Representative images of mice from each group.

(B–F) (B) Photographs, (C) weights, and (D) H&E staining of eWAT, iWAT and iBAT in the two groups. Images were taken at 10x magnification (Nikon Eclipse Ti confocal microscope). Adipocyte size distribution in (E) eWAT and (F) iWAT of *Mtp*<sup>f/f</sup> and *A-Mtp*<sup>-/-</sup> mice.

(G–I) MTP (G) mRNA and (H) protein levels. (I) Densitometry analysis of the blot shown in H, normalized to  $\beta$ -actin and plotted as fold change over the control.

(J–L) (J) Expression of genes involved in fatty acid oxidation. (K) *Pgc1α*, *Ucp1* and *Cpt1a* proteins in iWAT and iBAT of *Mtp*<sup>f/f</sup> and *A-Mtp*<sup>-/-</sup> mice. (L) Densitometry analysis of blots shown in K, normalized to  $\beta$ -actin (n = 6). Bars and error bars represent mean  $\pm$  SD, \**P* < 0.05, \*\**P* < 0.01 and \*\*\**P* < 0.001, multiple two-tailed unpaired *t*-test.

*Mttp*<sup>-/-</sup> and *Mttp*<sup>f/f</sup> mice kept at 23 °C and collected their blood before and 15 min after injections. *A-Mttp*<sup>-/-</sup> mice had significantly higher FFA levels than *Mttp*<sup>f/f</sup> mice before and after CL316243 stimulation (Fig. 3H). Because individual mice had different FFA levels before the injections, we subtracted the initial FFA levels from those after CL316243 challenge to calculate the increases in FFA in response to the challenge. Again, elevations in FFA levels in response to adrenergic stimuli were significantly more robust in *A-Mttp*<sup>-/-</sup> mice than *Mttp*<sup>f/f</sup> mice (Fig. 3I). Similar to male mice, female *A-Mttp*<sup>-/-</sup> mice had significantly higher fasting plasma FFA levels than *Mttp*<sup>f/f</sup> mice (Supplementary Fig. 7E). These results indicated that *A-Mttp*<sup>-/-</sup> mice show greater mobilization of FFA after  $\beta$ 3-adrenergic stimulation.

In short, these metabolic studies revealed that *A-Mttp*<sup>-/-</sup> mice, compared with *Mttp*<sup>f/f</sup> mice, show greater mobilization of adipose fat and spend more energy under stress. This physiological mechanism may contribute to reduced weight gain on an obesogenic diet.

### 3.4. *A-Mttp*<sup>-/-</sup> mice have smaller adipocytes and show greater expression of thermogenic genes than *Mttp*<sup>f/f</sup> mice at 23 °C

Since the physiological studies described above showed that *A-Mttp*<sup>-/-</sup> mice had less fat mass than *Mttp*<sup>f/f</sup> mice, we hypothesized that adipocyte phenotype would differ between the MTP deficient and control mice. To test this hypothesis, we sacrificed mice after 6 months on an obesogenic diet. Qualitative images showed that *A-Mttp*<sup>-/-</sup> mice were leaner than *Mttp*<sup>f/f</sup> mice (Fig. 4A). Representative images of eWAT, iWAT and iBAT demonstrated lower fat mass in male *A-Mttp*<sup>-/-</sup> mice (Fig. 4B). The weights of eWAT, iWAT and iBAT were significantly lower in *A-Mttp*<sup>-/-</sup> mice (Fig. 4C), and adipocytes in eWAT and iWAT of *A-Mttp*<sup>-/-</sup> mice were smaller than those in *Mttp*<sup>f/f</sup> mice (Fig. 4D–F), in agreement with previous studies [15,16]. As expected, the *A-Mttp*<sup>-/-</sup> mice had significantly lower MTP mRNA and protein levels in eWAT, iWAT and iBAT (Fig. 4G–I), but this was not observed in the liver and

intestines (Fig. 4H, I and Supplementary Fig. 8A), thus indicating that adipocyte-specific MTP deficiency does not result in compensatory changes in other tissues.

The smaller adipocytes might have been due to defects in adipogenesis, *de novo* lipogenesis and/or elevated fatty acid oxidation. We did not find differences in the expression of genes involved in adipogenesis (*Ppar $\gamma$* ) and lipogenesis (*Fas* and *Srebp1c*) in eWAT, iWAT and iBAT (Supplementary Fig. 8B–D). However, we observed greater mRNA and protein levels of thermogenic genes *Pgc1 $\alpha$* , *Ucp1* and *Cpt1 $\alpha$*  in the iWAT and iBAT in *A-Mttp*<sup>-/-</sup> mice than in *Mttp*<sup>f/f</sup> mice (Fig. 4J–L). Similarly, female *A-Mttp*<sup>-/-</sup> mice had smaller adipocytes in iWAT, and demonstrated elevated expression of thermogenic genes in iWAT and iBAT (Supplementary Fig. 9A–I). These results suggested that MTP deficiency in adipose tissue may not affect adipogenesis and lipogenesis, but may increase thermogenesis, thereby contributing to a smaller adipocyte size.

### 3.5. *A-Mttp*<sup>-/-</sup> mice show improved glucose tolerance and insulin sensitivity compared to *Mttp*<sup>f/f</sup> mice

Smaller adipocytes and increased thermogenesis are reported to have positive effects on glucose homeostasis [32,33]. To understand the physiological significance of smaller adipocytes and increased thermogenesis in *A-Mttp*<sup>-/-</sup> mice, we analyzed various parameters to assess glucose homeostasis. Intraperitoneal glucose tolerance test showed that *A-Mttp*<sup>-/-</sup> mice have better tolerance to glucose compared to *Mttp*<sup>f/f</sup> mice (Fig. 5A). We found that *A-Mttp*<sup>-/-</sup> mice on an obesogenic diet are more insulin sensitive compared to *Mttp*<sup>f/f</sup> mice (Fig. 5B, C). We also found that *A-Mttp*<sup>-/-</sup> mice have significantly lower fasting glucose (Fig. 5D), insulin (Fig. 5E), and HOMA-IR compared to *Mttp*<sup>f/f</sup> mice (Fig. 5F). The above results suggest that smaller adipocytes and increased thermogenesis resulting from the ablation of MTP in adipocytes has beneficial effects on whole body glucose homeostasis.

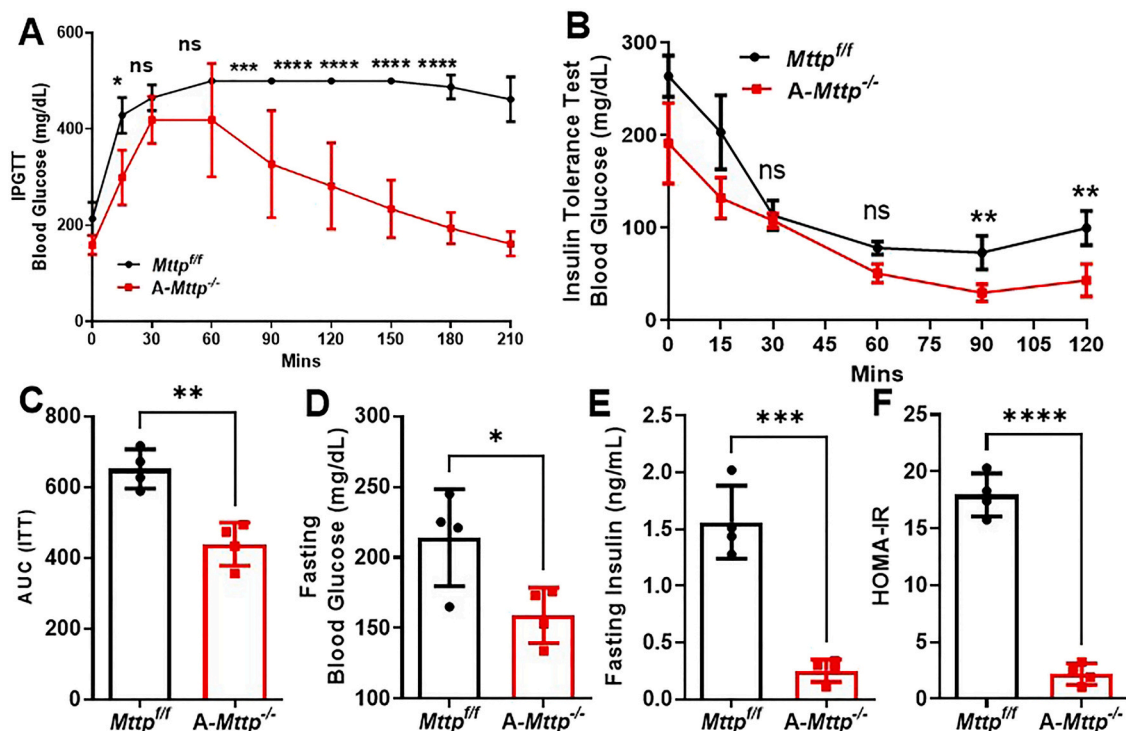


**Fig. 5.** *A-Mttp*<sup>-/-</sup> mice have better glucose tolerance compared to *Mttp*<sup>f/f</sup> mice. Male *Mttp*<sup>f/f</sup> and *A-Mttp*<sup>-/-</sup> mice (n = 4) fed an obesogenic diet for 6 months were fasted for 16 h and IP administered with (A) 2 g/kg of glucose to perform IPGTT or (B) 0.75 IU/Kg of insulin for ITT at different times. (C) Area under curve (AUC) of ITT. (D) Overnight fasting glucose levels, (E) fasting insulin levels (F) and HOMA-IR in *Mttp*<sup>f/f</sup> and *A-Mttp*<sup>-/-</sup> mice. The error bars represent mean  $\pm$  SD. Significance was calculated with two-way ANOVA followed by multiple comparisons in A and B. Student *t*-test was used to calculate the significance in graph C–F. \**P* < 0.05, \*\**P* < 0.01 and \*\*\**P* < 0.001.

### 3.6. Adipocytes differentiated from A-Mtp<sup>-/-</sup> mouse SVF show elevated triglyceride hydrolase activity

To understand the molecular mechanisms underlying the elevated thermogenesis in adipose tissue of A-Mtp<sup>-/-</sup> mice, we isolated the SVF from inguinal fat pads of Mtp<sup>f/f</sup> mice and A-Mtp<sup>-/-</sup> mice and differentiated them into adipocytes [18]. The cell proliferation was similar in Mtp<sup>f/f</sup> and A-Mtp<sup>-/-</sup> adipocytes at 24 h and 48 h (Supplementary Fig. 10A). After differentiation, Mtp<sup>f/f</sup> and A-Mtp<sup>-/-</sup> adipocytes demonstrated similar expression of genes associated with adipogenesis and lipogenesis (Supplementary Fig. 10B) indicating that MTP deficiency did not affect cell proliferation and adipogenesis. As expected, A-Mtp<sup>-/-</sup> adipocytes demonstrated significantly lower levels of MTP protein than Mtp<sup>f/f</sup> adipocytes (Fig. 6A). Oil red O staining and quantification indicated that A-Mtp<sup>-/-</sup> adipocytes accumulated less lipid than Mtp<sup>f/f</sup> adipocytes (Fig. 6B, C). A-Mtp<sup>-/-</sup> adipocytes on starvation secreted significantly higher FFA than Mtp<sup>f/f</sup> adipocytes (Fig. 6D). To test the hypothesis that this greater secretion might be due to increased lipolysis, we incubated cell lysates from Mtp<sup>f/f</sup> and A-Mtp<sup>-/-</sup> adipocytes with nitrobenzoxadiazole (NBD)-labeled TG and measured the FFA release over time [20]. A-Mtp<sup>-/-</sup> adipocytes demonstrated greater increases in NBD-labeled FFA release over time than Mtp<sup>f/f</sup> adipocyte cell lysates indicating elevated lipolysis (Fig. 6E). These results revealed that A-Mtp<sup>-/-</sup> adipocytes have higher amounts of TG hydrolase activity and mobilize more FFA than Mtp<sup>f/f</sup> adipocytes.

### 3.7. MTP deficiency in adipocytes increases lipolysis by ATGL

Two major lipases, adipose triglyceride lipase (ATGL) and hormone sensitive lipase (HSL) [34–38], hydrolyze TG stores in the adipose tissue. To identify the lipase(s) responsible for enhanced lipolysis in A-Mtp<sup>-/-</sup> adipocytes, we incubated cell lysates from A-Mtp<sup>-/-</sup> and Mtp<sup>f/f</sup> adipocytes with NBD-labeled TG in the presence or absence of ATGL (atlistatin, ATGLi) and HSL (SC206328, HSLi) inhibitors (Fig. 6F). A-Mtp<sup>-/-</sup> adipocytes showed significantly greater FFA release than Mtp<sup>f/f</sup> adipocytes. HSLi did not influence FFA release in Mtp<sup>f/f</sup> and A-Mtp<sup>-/-</sup> adipocytes (Fig. 6F). However, ATGLi significantly inhibited lipolysis in both Mtp<sup>f/f</sup> and A-Mtp<sup>-/-</sup> adipocyte lysates indicating that ATGL is the main enzyme responsible for TG lipolysis in adipocytes. We considered that the greater ATGL-mediated lipolysis in A-Mtp<sup>-/-</sup> adipocytes might be due to increased protein. However, ATGL protein levels did not differ between Mtp<sup>f/f</sup> and A-Mtp<sup>-/-</sup> adipocytes (Fig. 6G). Thus, A-Mtp<sup>-/-</sup> adipocytes had higher ATGL activity but similar protein levels indicating that MTP might modulate ATGL activity without affecting protein concentrations.

To address whether the MTP mediated inhibition of ATGL is tissue specific, we measured ATGL activity in the livers of Mtp<sup>f/f</sup> and liver-specific MTP knockout (L-Mtp<sup>-/-</sup>) mice generated by crossing Mtp<sup>f/f</sup> mice with Albumin<sup>Cre</sup> mice [6]. As expected, we found significantly decreased MTP protein and activity in livers of L-Mtp<sup>-/-</sup> mice compared to Mtp<sup>f/f</sup> mice (Supplementary Fig. 10C, D). Knockdown of MTP did not alter ATGL protein and activity in the livers of L-Mtp<sup>-/-</sup> mice (Supplementary Fig. 10C, E). These results suggest that MTP mediated inhibition of ATGL is specific to adipocytes. A reason for the inhibition of ATGL by MTP in the adipose tissue might be that adipocytes accumulate more lipid droplet and express high levels of ATGL compared to other tissues.

Increased ATGL-mediated TG hydrolysis increases FFA secretion and oxidation in adipocytes [38,39]. We previously showed that A-Mtp<sup>-/-</sup> adipocytes secrete more FFA than Mtp<sup>f/f</sup> adipocytes (Fig. 6D). Here, we addressed FFA oxidation and measured the oxygen consumption rate (OCR). A-Mtp<sup>-/-</sup> SVF differentiated white (Fig. 6H) and brown adipocyte (Supplementary Fig. 10F) demonstrated greater OCR than Mtp<sup>f/f</sup> adipocytes. To assess whether MTP deficiency related increases in OCR resulted from increased lipolysis by ATGL, we inhibited ATGL and HSL activity in A-Mtp<sup>-/-</sup> adipocytes. ATGLi decreased the OCR in A-Mtp<sup>-/-</sup>

adipocytes (Fig. 6I), whereas HSLi had no effect (Fig. 6J), thus indicating that A-Mtp<sup>-/-</sup> adipocytes require ATGL to increase OCR.

Next, we studied the effect of MTP deficiency in human adipocytes differentiated from SVF. siRNA mediated knockdown of MTP in human adipocytes, increased OCR to a greater extent than that of control adipocytes treated with siScramble (Fig. 6K) indicating that human MTP (hMTP) also regulates fatty acid oxidation. Furthermore, siRNA mediated knockdown of ATGL in siMTP treated adipocytes decreased OCR to a greater extent than that in siMTP only treated cells (Fig. 6L). Knockdown of HSL did not affect OCR in siMTP treated human adipocytes (Fig. 6M). These studies indicated that the increased FFA oxidation in MTP deficient adipocytes required ATGL activity and that hMTP also inhibits TG lipolysis by ATGL in human adipocytes.

### 3.8. The TG transfer activity of MTP is not essential for the inhibition of ATGL activity

TG is a common substrate for ATGL and MTP, and both proteins are on the LD surface (Fig. 1B) [14], therefore we hypothesized that MTP may compete with ATGL for TG and decrease hydrolysis. To test this possibility, we studied the effects of WT and the missense N780Y mutant MTP on ATGL activity. The N780Y mutation in abetalipoproteinemia patients significantly decreases TG transfer activity [40–42]. We hypothesized that if MTP competes for TG substrate with ATGL, then WT MTP would decrease ATGL activity, whereas the N780Y mutated form of MTP would not. We co-transfected Cos-7 cells with plasmids for expression of human ATGL (hATGL-His) [19] with either MTP-Flag or N780Y-Flag (Fig. 7A) and subsequently measured MTP's TG transfer activity (Fig. 7B) and ATGL's TG hydrolase activity (Fig. 7C). Expression of hMTP significantly increased the TG transfer activity (Fig. 7B). As expected, lysates of N780Y expressing Cos-7 cells showed significantly less TG transfer activity (Fig. 7B). Similarly, ATGL-His expressing cells demonstrated very little TG transfer activity, similar to control pcDNA3 and N780Y expressing cells indicating that ATGL does not transfer TG (Fig. 7B). Cells co-expressing ATGL and MTP showed TG transfer activity similar to MTP expressing cells indicating that ATGL has no effect on MTP's TG transfer activity (Fig. 7B).

We next studied the effect of MTP on ATGL activity. Expression of either WT or N780Y MTP did not increase FFA release, indicating that these proteins lack TG hydrolase activity (Fig. 7C). As expected, hATGL-His expressing cell lysates showed higher FFA release than pcDNA3 expressing cells indicating greater lipolysis (Fig. 7C). Co-expression of either MTP or N780Y with ATGL significantly decreased FFA release (Fig. 7C). These studies demonstrated that ATGL expression increases lipolysis, and that the expression of MTP and N780Y significantly decreases ATGL activity. Therefore, MTP inhibits ATGL activity, and this inhibition is independent of MTP's TG transfer activity.

To provide further evidence, we expressed MTP-Flag and N780Y-Flag and purified these proteins. As expected, purified N780Y had much less TG transfer activity than MTP (Fig. 7D). We used these purified proteins to study their effects on purified mouse ATGL (mATGL) activity in the presence or absence of CGI-58, an activator of ATGL [19,43]. As expected, purified ATGL showed substantial TG hydrolysis, and this activity increased by ~10-fold in the presence of CGI-58 (Fig. 7E). More importantly, addition of both WT and N780Y MTP decreased ATGL activity both in the presence and absence of CGI-58 (Fig. 7E). Moreover, MTP and N780Y proteins showed dose-dependent inhibition of ATGL activity (Fig. 7F). In short, these results showed that both WT and mutant MTP proteins inhibit TG lipolysis by ATGL and ATGL/CGI-58. Therefore, inhibition of ATGL by MTP does not require TG transfer activity, implying that competition for substrate is not a major mode of inhibition.

### 3.9. MTP interacts with ATGL

We then hypothesized that MTP might physically interact with ATGL

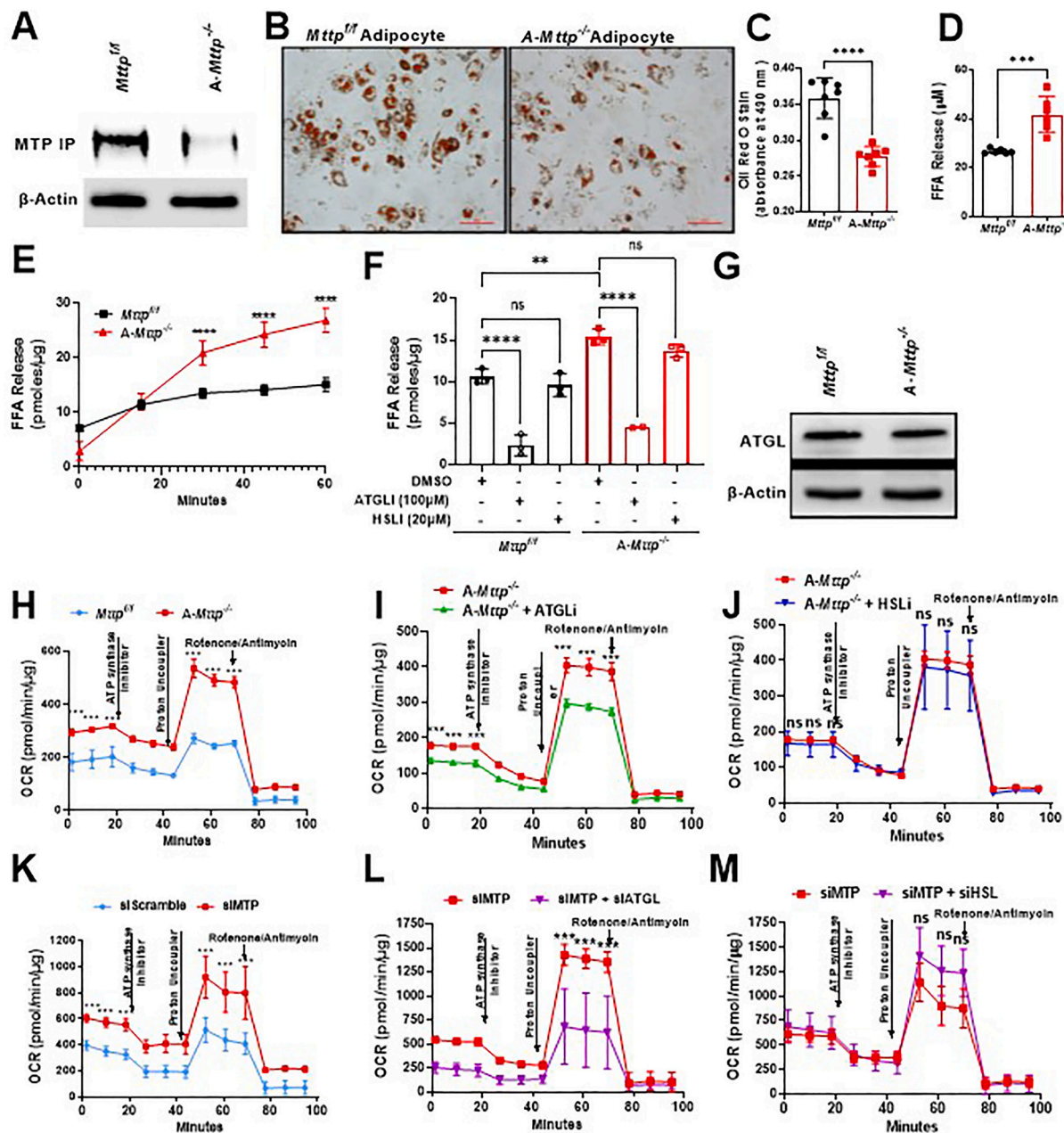


**Fig. 6.** Adipocytes differentiated from A-Mtp<sup>-/-</sup> mouse SVF show elevated triglyceride hydrolase activity.

(A) iWAT was collected from Mtp<sup>f/f</sup> and A-Mtp<sup>-/-</sup> mice (n = 3), and SVF was isolated and differentiated into adipocytes to measure MTP protein levels. Representative of two experiments.

(B–C) (B) Oil red O staining of adipocytes differentiated from Mtp<sup>f/f</sup> and A-Mtp<sup>-/-</sup> SVF (10× magnification using confocal microscope). (C) Adipocytes were stained with Oil red O (n = 7), the stain was extracted, and the absorbance was determined at 490 nm. Representative of two experiments.

(D) Differentiated adipocytes were washed and incubated for 3 h in PBS containing 0.1 % BSA and FFA were measured in medium. Representative of two experiments.

(E) Mtp<sup>f/f</sup> and A-Mtp<sup>-/-</sup> adipocyte cell lysates (100 μl, 30 μg) were incubated with NBD labeled TG vesicles (10 μl, 3155 pmol) and NBD fluorescence was measured at different time points for 1 h. FFA release was calculated with an NBD-C6 standard curve. Representative of four experiments.

(F) Cell lysates (100 μl, 30 μg) from Mtp<sup>f/f</sup> and A-Mtp<sup>-/-</sup> adipocytes were incubated with NBD labeled TG vesicles (10 μl, 3155 pmol) in the presence of DMSO, ATGLi (100 μM) or HSLi (20 μM) for 1 h. Representative of four experiments.

(G) ATGL protein cell lysates of Mtp<sup>f/f</sup> and A-Mtp<sup>-/-</sup> in white adipocytes.

(H–J) (H) Measurement of OCR in adipocytes differentiated from Mtp<sup>f/f</sup> and A-Mtp<sup>-/-</sup> SVF. Adipocytes in basal low glucose medium were treated with (I) ATGLi, (J) HSL or vehicle. Representative of two experiments.

(K–M) OCR in adipocytes differentiated from human SVF. (K) Human adipocytes were transfected with scrambled siRNA (siScramble) or siMTP. (L) Adipocytes were transfected with siMTP or siMTP+siATGL. (M) Cells were transfected with siMTP with or without siHSL. Representative of two experiments.

The error bars represent SD (n = 3–5). Two-way ANOVA followed by multiple comparison in E, H, I, J, K, L and M. In F, one-way ANOVA followed by multiple comparison was performed. Student's t-test was used for C and D. \*P < 0.05, \*\*P < 0.01, \*\*\*P < 0.001, and \*\*\*\*P < 0.0001. (For interpretation of the references to color in this figure legend, the reader is referred to the web version of this article.)

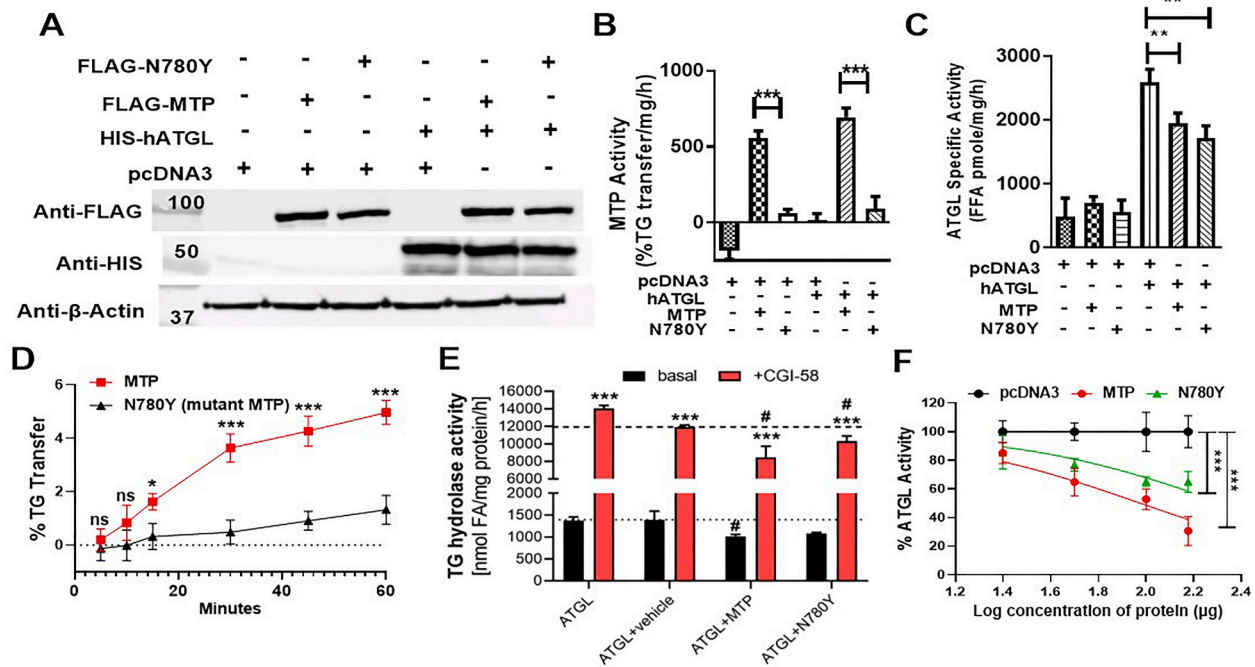


**Fig. 7.** The TG transfer activity of MTP is not essential for the inhibition of ATGL activity.

(A–C) Cos-7 cells were seeded in 150 mm cell culture dishes and forward transfected with 30  $\mu$ g pcDNA3 or His-tagged ATGL. After 24 h, cells were trypsinized, plated in 100 mm cell culture dishes, and reverse transfected in triplicate with 7.5  $\mu$ g of pcDNA3, Flag-tagged MTP or mutant N780Y. After 48 h, cells were lysed, and protein was used for experiments. (A) Protein (20  $\mu$ g) was analyzed with SDS-PAGE and probed with anti-FLAG, anti-His and anti- $\beta$ -Actin antibodies. Protein (100  $\mu$ g) was used for (B) MTP and (C) ATGL activity measurements.

(D) MTP-Flag and N780Y-Flag proteins were purified to measure the TG transfer activity.

(E) TG hydrolase activity of purified ATGL with or without CGI-58 in the presence of purified MTP and N780Y.

(F) Cos-7 cells were transfected with Flag-tagged MTP, N780Y or His-tagged ATGL. Lysates of ATGL expressing Cos-7 cells (50  $\mu$ g) were mixed with 25, 50, 100 or 150  $\mu$ g of lysates of MTP and N780Y expressing cells and incubated with 10  $\mu$ l (3155 pmol) of NBD-TAG PC/PI vesicles for 1 h. FFA was extracted after 1 h incubation, and NBD fluorescence readings were taken.

The graphs in B, C and F are representative of three experiments with three biological replicates. Graph E is representative of two independent experiments, each containing three biological replicates. The error bars represent SD. Significance was calculated with one-way ANOVA followed by multiple comparisons in D and F with two-way ANOVA followed by multiple comparison for B, C and E. \* $P < 0.05$ , \*\* $P < 0.01$  and \*\*\* $P < 0.001$ .

and inhibit its activity. To test this hypothesis, we used lysates from human adipocytes differentiated from SVF and immunoprecipitated using anti-CGI-58 and anti-MTP antibodies. Mouse and rabbit IgGs were used as negative controls and anti-CGI-58 was used as a positive control. The immunoprecipitated proteins were separated on SDS-PAGE and probed with anti-CGI-58, anti-MTP and anti-ATGL. We found that ATGL was present in both CGI-58 and MTP immunoprecipitates (Fig. 8A) indicating that ATGL interacts with both MTP and CGI-58. Next, we expressed Flag-tagged MTP [40,41] and CGI-58 [19] in Cos-7 cells, purified these proteins (Fig. 8B) and immobilized them on plates to study protein-protein interactions as previously described [10,19,44,45]. For controls, BSA and FLAG peptide were coated in parallel. These wells were then incubated with lysates expressing His-tagged human ATGL (hATGL), mATGL or mHSL (Fig. 8B). Lysates of hATGL and mATGL expressing cells showed greater binding to immobilized MTP and N780Y than the background binding to BSA and FLAG (Fig. 8C, D). As reported earlier [19,43], cell lysates expressing hATGL and mATGL showed greater binding to CGI-58 (Fig. 8C, D); in contrast, HSL expressing cell lysates did not show greater binding to immobilized purified MTP, N780Y and CGI-58 than to BSA and FLAG control wells (Fig. 8E). Moreover, hATGL and mATGL showed a concentration dependent increased binding to immobilized MTP, N780Y and CGI-58, while HSL did not (Supplementary Fig. 11A–C). These studies indicated that both MTP and N780Y interact with ATGL but not with HSL.

To further validate the interaction between MTP and ATGL, we co-expressed Xpress-tagged human ATGL (hATGL), mouse ATGL (mATGL), or a truncated mATGL variant lacking 198C-terminal amino

acids (mATGL 288\*) along with either Flag-tagged MTP, CGI58 or empty Flag (eFlag) in HEK-293 T cells. The mATGL 288\* has been shown to retain TG hydrolase activity and it interacts with CGI-58 and G0S2 [46–48]. These proteins, respectively, enhance and reduce ATGL activity. The Flag-tagged bait proteins were successfully expressed (Fig. 8F, left) and immunoprecipitated using anti-Flag affinity gel (Fig. 8F, right). Expression of the Xpress-tagged ATGL variants was confirmed using an anti-Xpress antibody (Fig. 8G, left). Notably, hATGL and mATGL not only co-precipitated with Flag-CGI-58 (positive control) but also with Flag-MTP (Fig. 8G, right). This indicates that both the human and mouse orthologs of ATGL interact with MTP in cell lysates. In contrast, mATGL288\* co-precipitated to a lesser extent with Flag-MTP than full-length mATGL indicative for a decreased binding affinity of mATGL288\* to MTP. Importantly, mATGL did not precipitate in absence of flag-tagged bait proteins excluding non-specific binding to the anti-Flag affinity gel. These results demonstrated that MTP physically interacts with ATGL, and this interaction might serve as the mechanism for the inhibition of ATGL activity.

#### 4. Discussion

MTP's best-characterized function is to lipidate nascent proteins in the endoplasmic reticulum of hepatocytes, enterocytes and antigen presenting cells. This function is dependent on MTP's ability to transfer lipids, given that mutations resulting in the loss of lipid transfer activity fail to lipidate apoB and CD1 proteins in abetalipoproteinemia subjects [2,49]. In this study, we showed that human adipocytes express MTP

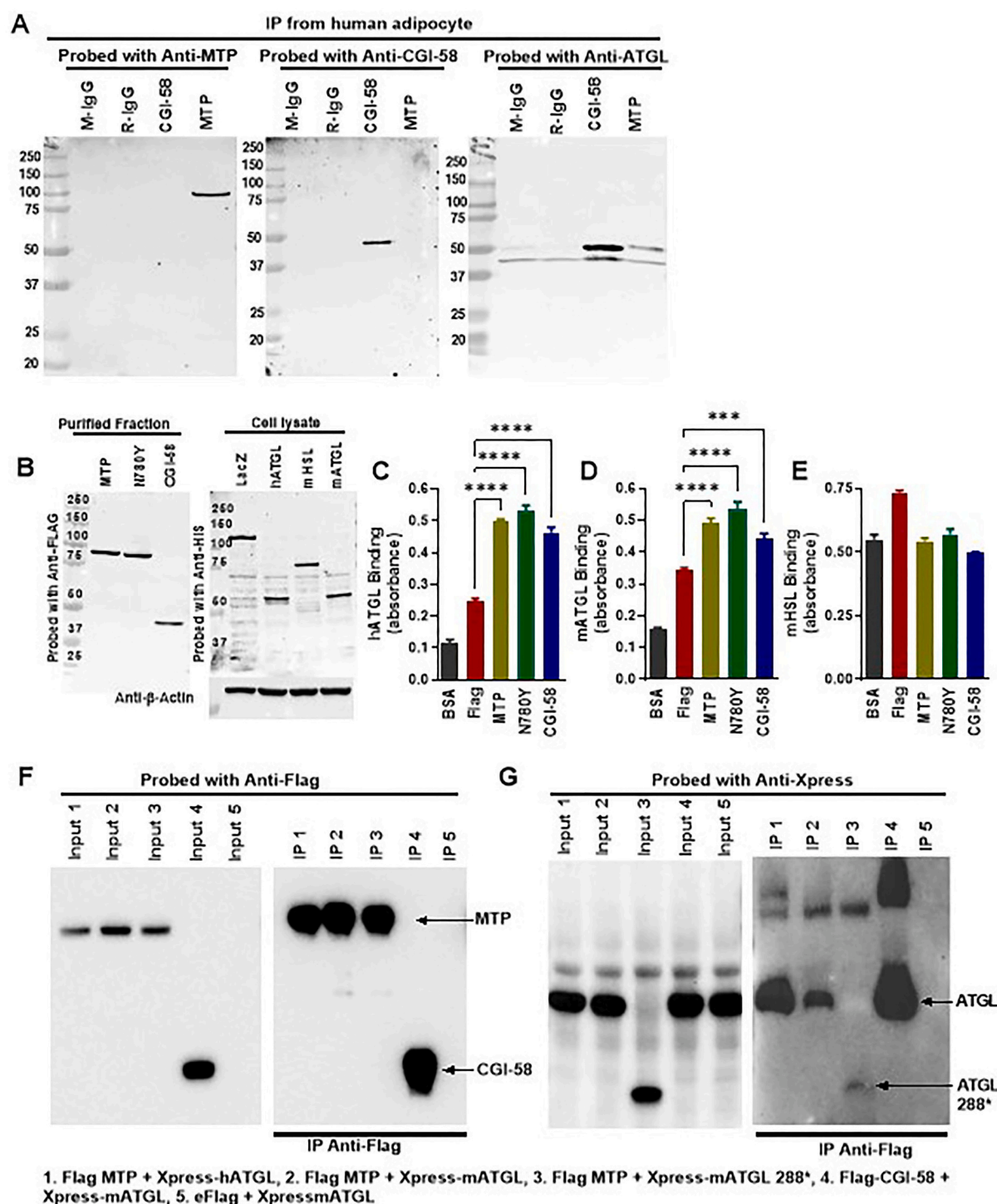


**Fig. 8.** MTP interacts with ATGL.

(A) Human adipocytes differentiated from SVF were lysed and 400  $\mu$ g of protein was used for immunoprecipitation with mouse IgG, rabbit IgG, anti-CGI58 and anti-MTP. The immunoprecipitated proteins were separated on SDS PAGE and probed with anti-CGI58, anti-MTP and anti-ATGL.

(B–E) Cos-7 cells were transfected, and Flag-tagged MTP, N780Y and CGI proteins were purified. High binding plates were coated with purified proteins and incubated with Cos-7 cell lysates expressing His-tagged (C) hATGL, (D) mATGL or (E) mHSL. Binding of proteins was detected with anti-His primary antibody and secondary antibody conjugated with horseradish peroxidase. The absorbance of the peroxidase reaction was determined at 450 nm. The data are representative of three to five experiments, each with three biological replicates. One-way ANOVA followed by multiple comparison in B, C and D. \*\*\*\* $P < 0.0001$ .

(F–G) HEK293T cells transfected with the indicated plasmid combinations and the respective lysates were subjected to co-immunoprecipitation using anti-Flag affinity gel. (F) Proper expression (left) and precipitation (right) of bait proteins was verified by immunoblotting using an anti-Flag antibody. (G) Proper expression (left) and co-precipitation (right) of prey proteins was verified by immunoblotting using an anti-Xpress antibody.

and is present on lipid droplets. Furthermore, we demonstrated that highly selective adipose-specific MTP deficiency confers resistance to weight gain, helps maintain higher body temperature during cold challenge, and enhances lipolysis and mobilization of FFA in mice fed an obesogenic diet. Thus, *A-Mtp*<sup>-/-</sup> mice adapt better than controls during stress conditions. Our mechanistic studies also revealed that MTP regulates lipolysis in adipocytes by inhibiting ATGL activity. This regulatory activity of MTP does not require its lipid transfer activity. Thus, MTP, independent of its lipid transfer function, regulates fat mobilization and thermogenesis in adipocytes.

Further molecular studies revealed that MTP inhibits ATGL activity via protein-protein interactions. Attempts were made to identify domains in ATGL that interact with MTP. Based on the analyses of mutations found in humans, mutagenesis studies and homology remodeling, it has been proposed that ATGL contains structurally independent domains that carry out distinct functions [46,47]. The N-terminal domain (1–254 amino acids) contains the enzymatically active patatin domain [46]. The C-terminal domain (amino acids 250–504 amino acids) consists of  $\alpha$ -helices and loop regions [47,48]. It contains a hydrophobic stretch (315–360 amino acids) potentially representing lipid-binding region. Schweiger et al. showed that N-terminal domain, lacking C-terminal ~220 amino acids, does not localize to lipid droplets [46]. However, this N-terminal domain exhibits substantially increased TG hydrolase activity suggesting that the C-terminal domain suppresses enzyme activity of the N-terminal domain [46]. Furthermore, the N-terminal protein interacts with CGI-58 and G0S2 [47] to enhance and reduce ATGL activity, respectively. Schweiger et al. further showed that the N- and C-terminal domains can be swapped within mouse and human ATGL [46] providing additional evidence that these proteins contain two independent functional domains with distinct functions. The N-terminal domain contains TG hydrolase activity and is involved in protein-protein interactions with CGI-58 and G0S2 proteins [46,47]. The C-terminal domain interferes with the enzyme activity and is important for lipid droplet association. Based on these studies, we used N-terminal ATGL 288\* to determine whether this domain also interacts with MTP. We observed that C-terminally truncated N-terminal ATGL 288\* interacted less efficiently than the WT ATGL indicating that MTP might interact with the C-terminal domain of ATGL. We speculate that the C-terminal domain of ATGL may interact with the N-terminal and/or central  $\alpha$ -helical domains of MTP. Further studies are needed to understand determinants of protein-protein interactions between MTP and ATGL.

When compared with controls, we showed that adipose MTP deficiency confers better thermoregulation during a cold challenge, as well as decreased weight gain on an obesogenic diet. *A-Mtp*<sup>-/-</sup> mice showed elevated plasma FFA. Furthermore, *A-Mtp*<sup>-/-</sup> mice showed increased expression of thermogenic genes in iWAT and iBAT, suggesting greater utilization of fatty acids. This largely favorable phenotype might be secondary to the identified MTP function in inhibiting ATGL activity. ATGL is the rate limiting lipase catalyzing the initial step of TG hydrolysis [34]. ATGL deficient mice do not adapt well to cold challenge [39,50,51]. In contrast, overexpression of ATGL in adipose tissue decreases adipocyte TG content, increases thermogenesis and energy expenditure in mice, and these mice gain less weight than wild type mice on an obesogenic diet [52]. Thus, our studies suggest that MTP might play a significant role in the control of thermogenesis by modulating ATGL activity.

The lipolytic activity of ATGL is regulated by both transcriptional and post-translational mechanisms [38]. The post-translational mechanisms involve the interaction of ATGL with different regulatory peptides. Both activity enhancing and inhibiting proteins have been identified [38,53,54]. These regulatory proteins, in general, physically interact with ATGL and consequently increase or decrease its activity. Most of the identified regulatory proteins are small polypeptides of 60–350 amino acids. Here, we show that MTP, a heterodimer of 150 kDa and 97 kDa proteins, interacts with ATGL and inhibits its activity. The

physiological role of most of the identified ATGL inhibitory peptides is unclear, as their deficiencies show modest to no effects on lipolysis, lipid and energy metabolism, and adipose tissue morphology [38]. In contrast, our studies show that adipose specific MTP deficiency had significant effects on lipolysis, lipid mobilization, energy metabolism and adipocyte size. Thus, adipose MTP may be a physiologically noteworthy modulator of ATGL activity and adipocyte triglyceride homeostasis.

Our results indicate that the interaction and inhibition of ATGL by MTP might be specific to adipose tissue as the ablation of MTP in the liver did not increase liver ATGL activity. The lack of effect of MTP deficiency on hepatic ATGL might be related to their different sub-cellular localization and engagement of MTP with apoB in the endoplasmic reticulum of hepatocytes. We speculate that specific interactions between MTP and ATGL might occur on the lipid droplet surface in adipocytes, and that the larger and greater number of lipid droplets in adipocyte cytoplasm increases the likelihood of protein-protein interactions between ATGL and MTP.

It is well known that MTP plays a critical role in the mobilization of dietary and endogenous fat by the intestine and liver, respectively. Our current studies suggest that adipose MTP may play a role in fat storage. Under the conditions of high fat absorption by the intestine and subsequent mobilization by the liver, peripheral tissues are exposed to high plasma triglyceride and free fatty acids. This might lead to excess ectopic accumulation in peripheral tissues, such as liver, heart and muscle contributing to metabolic diseases. To avoid ectopic fat deposition in other tissues, adipose tissue performs a unique function of storing large amounts of fat in an innocuous form. It appears that MTP has acquired a different function in the adipose tissue to facilitate fat storage that is very different than its function of fat mobilization in the liver and intestine. By performing these two contrasting activities in different tissues, MTP can regulate body fat metabolism to optimize its delivery to fat-consuming/storing tissues and avoid ectopic fat deposition.

We have used two different high fat diets. The western diet contains 43 % fat whereas obesogenic diet contains 60 % fat. The western diet also contains 0.2 % cholesterol and is usually used to induce atherosclerosis. We saw significant differences in weight gain when mice were fed an obesogenic diet indicating that MTP might be critical under these conditions. It is likely that Western diet fed mice have sufficient storage/expansion capacity that it might not need MTP to inhibit ATGL activity. On the other hand, in obesogenic diet, MTP is critical in facilitating adipose fat storage in adipose tissue to prevent fat storage in other tissues such as in the liver to avoid development of hepatosteatosis and other metabolic diseases associated with ectopic fat deposition. Thus, MTP may respond differently under different dietary conditions to regulate fat metabolism in the body.

Accumulation of lipids in intracellular LDs is seen in organisms as ancient as prokaryotes. These LDs act as hubs for metabolism, signaling, stress responses and membrane remodeling [55]. LD associated proteins such as CGI-58 and ATGL are present in lower organisms. MTP orthologs are present in invertebrates such as *C. elegans* [56] and can serve to transfer phospholipids [57,58]; however, MTP's TG transfer activity was acquired during the evolution of vertebrates [56]. Our present studies demonstrating MTP interactions with ATGL suggest that MTP might have evolved as an ATGL interacting protein before the acquisition of the TG transfer activity. We speculate that MTP is also likely to interact with other proteins in adipose tissue to modulate lipolysis and thermogenesis.

The obesity and cardio-metabolic disease epidemics are major causes of high morbidity and mortality. Adipose tissue plays a central role in the pathology of these diseases. Increasing the thermogenic activity of adipose tissue has been proposed as a promising strategy to combat both metabolic diseases and obesity [59]. Our data showed that MTP deficiency leads to smaller adipocytes, less weight gain, increased thermogenesis and enhanced insulin sensitivity. Furthermore, these promising characteristics help maintain body temperature by mobilizing fatty

acids during stress. Thus, adipose specific inhibition of MTP-ATGL protein-protein interactions may provide an avenue for future therapeutic targeting.

In brief, we demonstrated that adipose MTP plays an important role in the control of body temperature, thermogenesis and weight gain. In adipocytes, MTP has a unique function in interacting with ATGL and inhibiting its activity that is independent of its lipid transfer activity. This regulatory function of MTP is physiologically important in lipid metabolism and thermogenesis in adipose tissue under stress conditions. Inhibition of MTP-ATGL interactions might prevent obesity.

### CRedit authorship contribution statement

SR designed and performed experiments and wrote the manuscript. PH designed and performed ATGL hydrolysis assays and interaction studies. AC helped in mice studies and generated data. MS collected organs and processed the samples. LR designed the *in vivo* studies. EVC assisted in writing the manuscript and provided input. SKF discussed FFA release studies and various experiments. RL and CB obtained human adipose tissue and helped in writing the manuscript. RZ planned TG hydrolysis experiments by ATGL and assisted in writing the manuscript. GJS planned and performed thermoneutral and cold challenge experiments and extensively discussed results. MMH conceptualized the idea, provided funding, oversaw the progress and wrote the manuscript. All authors have read the manuscript and provided comments.

### Funding and additional information

This work was supported in part by the U.S. National Institutes of Health grants DK121490, HL137202, HL158054 and HD094778; VA Merit Award BX004113 to MMH; American Heart Association Award 19POST34410063 to SR; and The Austrian Science Fund grant F73 SFB Lipid Hydrolysis awarded to RZ. The contents of this article are solely the responsibility of the authors and do not represent the official views of the NIH, the Department of Veterans Affairs or the U.S. Government. We acknowledge the assistance of Veronica Denig in animal care.

### Appendix A. Supplementary data

Supplementary data to this article can be found online at <https://doi.org/10.1016/j.metabol.2022.155331>.

### References

- [1] Hussain MM, Shi J, Dreizen P. Microsomal triglyceride transfer protein and its role in apolipoprotein B-lipoprotein assembly. *J Lipid Res* 2003;44:22–32.
- [2] Wetterau JR, Aggerbeck LP, Bouma ME, Eisenberg C, Munck A, Hermier M, et al. Absence of microsomal triglyceride transfer protein in individuals with abetalipoproteinemia. *Science* 1992;258:999–1001.
- [3] Rader DJ, Kastelein JJ. Lomitapide and mipomersen: two first-in-class drugs for reducing low-density lipoprotein cholesterol in patients with homozygous familial hypercholesterolemia. *Circulation* 2014;129:1022–32.
- [4] Berberich AJ, Hegele RA. Lomitapide for the treatment of hypercholesterolemia. *Expert Opin Pharmacother* 2017;18:1261–8.
- [5] Cuchel M, Bloedon LT, Szapary PO, Kolansky DM, Wolfe ML, Sarkis A, et al. Inhibition of microsomal triglyceride transfer protein in familial hypercholesterolemia. *N Engl J Med* 2007;356:148–56.
- [6] Iqbal J, Walsh MT, Hammad SM, Cuchel M, Tarugi P, Hegele RA, et al. Microsomal triglyceride transfer protein transfers and determines plasma concentrations of ceramide and sphingomyelin but not glycosylceramide. *J Biol Chem* 2015;290:25863–75.
- [7] Brozovic S, Nagaishi T, Yoshida M, Betz S, Salas A, Chen DH, et al. CD1d function is regulated by microsomal triglyceride transfer protein. *Nat Med* 2004;10:535–9.
- [8] Bradbury P, Mann CJ, Kochl S, Anderson TA, Chester SA, Hancock JM, et al. A common binding site on the microsomal triglyceride transfer protein for apolipoprotein B and protein disulfide isomerase. *J Biol Chem* 1999;274:3159–64.
- [9] Bakillah A, Hussain MM. Binding of microsomal triglyceride transfer protein to lipid vesicles results in increased affinity for apolipoprotein B: identification of novel, intracellular MTP/lipid complexes. *Circulation* 1999;100:3934.
- [10] Hussain MM, Bakillah A, Nayak N, Shelness GS. Amino acids 430–570 in apolipoprotein B are critical for its binding to microsomal triglyceride transfer protein. *J Biol Chem* 1998;273:25612–5.
- [11] Dougan SK, Rava P, Hussain MM, Blumberg RS. MTP regulated by an alternate promoter is essential for NKT cell development. *J. Exp. Med.* 2007;204:533–45.
- [12] Dougan SK, Salas A, Rava P, Agyemang A, Kaser A, Morrison J, et al. Microsomal triglyceride transfer protein lipidation and control of CD1d on antigen-presenting cells. *J Exp Med* 2005;202:529–39.
- [13] Swift LL, Kakkad B, Boone C, Jovanovska A, Jerome WG, Mohler PJ, et al. Microsomal triglyceride transfer protein expression in adipocytes: a new component in fat metabolism. *FEBS Lett* 2005;579:3183–9.
- [14] Love JD, Suzuki T, Robinson DB, Harris CM, Johnson JE, Mohler PJ, et al. Microsomal triglyceride transfer protein (MTP) associates with cytosolic lipid droplets in 3T3-L1 adipocytes. *PLoS One* 2015;10:e0135598.
- [15] Bakillah A, Hussain MM. Mice subjected to ap2-cre mediated ablation of microsomal triglyceride transfer protein are resistant to high fat diet induced obesity. *Nutr Metab (Lond)* 2016;13:1.
- [16] Swift LL, Love JD, Harris CM, Chang BH, Jerome WG. Microsomal triglyceride transfer protein contributes to lipid droplet maturation in adipocytes. *PLoS One* 2017;12:e0181046.
- [17] Rajan S, Satish S, Shankar K, Pandeti S, Varshney S, Srivastava A, et al. Aegeline inspired synthesis of novel beta3-AR agonist improves insulin sensitivity in vitro and in vivo models of insulin resistance. *Metabolism* 2018;85:1–13.
- [18] Rajan S, Shankar K, Beg M, Varshney S, Gupta A, Srivastava A, et al. Chronic hyperinsulinemia reduces insulin sensitivity and metabolic functions of brown adipocyte. *J Endocrinol* 2016;230:275–90.
- [19] Lass A, Zimmermann R, Haemmerle G, Riederer M, Schoiswohl G, Schweiger M, et al. Adipose triglyceride lipase-mediated lipolysis of cellular fat stores is activated by CGI-58 and defective in chandler-dorfman syndrome. *Cell Metab* 2006;3:309–19.
- [20] Rajan S, de Guzman HC, Palaia T, Goldberg IJ, Hussain MM. A simple, rapid, and sensitive fluorescence-based method to assess triacylglycerol hydrolase activity. *J Lipid Res* 2021;62:100115.
- [21] Schweiger M, Eichmann TO, Taschler U, Zimmermann R, Zechner R, Lass A. Measurement of lipolysis. *Methods Enzymol* 2014;538:171–93.
- [22] Rajan S, Panzade G, Srivastava A, Shankar K, Pandey R, Kumar D, et al. miR-876-3p regulates glucose homeostasis and insulin sensitivity by targeting adiponectin. *J Endocrinol* 2018;239:1–17.
- [23] Gupta A, Singh VK, Kumar D, Yadav P, Kumar S, Beg M, et al. Curcumin-3,4-dichloro phenyl pyrazole (CDPP) overcomes curcumin's low bioavailability, inhibits adipogenesis and ameliorates dyslipidemia by activating reverse cholesterol transport. *Metabolism* 2017;73:109–24.
- [24] Grabner GF, Guttenberger N, Mayer N, Migglautsch-Sulzer AK, Lembacher-Fadum C, Fawzy N, et al. Small-molecule inhibitors targeting lipolysis in human adipocytes. *J Am Chem Soc* 2022;144:6237–50.
- [25] Athar H, Iqbal J, Jiang XC, Hussain MM. A simple, rapid, and sensitive fluorescence assay for microsomal triglyceride transfer protein. *J Lipid Res* 2004;45:764–72.
- [26] Rava P, Athar H, Johnson C, Hussain MM. Transfer of cholesteryl esters and phospholipids as well as net deposition by microsomal triglyceride transfer protein. *J Lipid Res* 2005;46:1779–85.
- [27] Fischer AW, Cannon B, Nedergaard J. Optimal housing temperatures for mice to mimic the thermal environment of humans: an experimental study. *Mol Metab.* 2018;7:161–70.
- [28] Reitman ML. Of mice and men - environmental temperature, body temperature, and treatment of obesity. *FEBS Lett* 2018;592:2098–107.
- [29] Shin H, Ma Y, Chanturiya T, Cao Q, Wang Y, Kadegowda AKG, et al. Lipolysis in Brown adipocytes is not essential for cold-induced thermogenesis in mice. *Cell Metab* 2017;26(764–77):e5.
- [30] Schreiber R, Diwoky C, Schoiswohl G, Feiler U, Wongsiriroj N, Abdellatif M, et al. Cold-induced thermogenesis depends on ATGL-mediated lipolysis in cardiac muscle, but not Brown adipose tissue. *Cell Metab* 2017;26(753–63):e7.
- [31] Preite NZ, Nascimento BP, Muller CR, Americo AL, Higa TS, Evangelista FS, et al. Disruption of beta3 adrenergic receptor increases susceptibility to DIO in mouse. *J Endocrinol* 2016;231:259–69.
- [32] Fan H, Zhang Y, Zhang J, Yao Q, Song Y, Shen Q, et al. Cold-inducible Klf9 regulates thermogenesis of Brown and Beige fat. *Diabetes* 2020;69:2603–18.
- [33] Rosen ED, Spiegelman BM. Adipocytes as regulators of energy balance and glucose homeostasis. *Nature* 2006;444:847–53.
- [34] Zimmermann R, Strauss JG, Haemmerle G, Schoiswohl G, Birner-Gruenberger R, Riederer M, et al. Fat mobilization in adipose tissue is promoted by adipose triglyceride lipase. *Science* 2004;306:1383–6.
- [35] Zechner R, Zimmermann R, Eichmann TO, Kohlwein SD, Haemmerle G, Lass A, et al. FAT SIGNALS - lipases and lipolysis in lipid metabolism and signaling. *Cell Metab* 2012;15:279–91.
- [36] Zechner R. FAT FLUX: enzymes, regulators, and pathophysiology of intracellular lipolysis. *EMBO Mol Med* 2015;7:359–62.
- [37] Recazens E, Mouiel E, Langin D. Hormone-sensitive lipase: sixty years later. *Prog Lipid Res* 2021;82:101084.
- [38] Grabner GF, Xie H, Schweiger M, Zechner R. Lipolysis: cellular mechanisms for lipid mobilization from fat stores. *Nat Metab.* 2021;3:1445–65.
- [39] Schoiswohl G, Stefanovic-Racic M, Menke MN, Wills RC, Surlow BA, Basantani MK, et al. Impact of reduced ATGL-mediated adipocyte lipolysis on obesity-associated insulin resistance and inflammation in male mice. *Endocrinology* 2015;156:3610–24.
- [40] Khatun I, Walsh MT, Hussain MM. Loss of both phospholipid and triglyceride transfer activities of microsomal triglyceride transfer protein in abetalipoproteinemia. *J Lipid Res* 2013;54:1541–9.
- [41] Walsh MT, Iqbal J, Josekutty J, Soh J, Di Leo E, Ozaydin E, et al. Novel abetalipoproteinemia missense mutation highlights the importance of the N-

- terminal beta-barrel in microsomal triglyceride transfer protein function. *Circ Cardiovasc Genet* 2015;8:677–87.
- [42] Read J, Anderson TA, Ritchie PJ, Vanloo B, Amey J, Levitt D, et al. A mechanism of membrane neutral lipid acquisition by the microsomal triglyceride transfer protein. *J Biol Chem* 2000;275:30372–7.
- [43] Gruber A, Cornaciu I, Lass A, Schweiger M, Poeschl M, Eder C, et al. The N-terminal region of comparative gene identification-58 (CGI-58) is important for lipid droplet binding and activation of adipose triglyceride lipase. *J Biol Chem* 2010;285:12289–98.
- [44] Bakillah A, Hussain MM. Binding of microsomal triglyceride transfer protein to lipids results in increased affinity for apolipoprotein B: evidence for stable microsomal MTP-lipid complexes. *J Biol Chem* 2001;276:31466–73.
- [45] Hofer P, Boeszoermenyi A, Jaeger D, Feiler U, Arthanari H, Mayer N, et al. Fatty acid-binding proteins interact with comparative gene Identification-58 linking lipolysis with lipid ligand shuttling. *J Biol Chem* 2015;290:18438–53.
- [46] Schweiger M, Schoiswohl G, Lass A, Radner FP, Haemmerle G, Malli R, et al. The C-terminal region of human adipose triglyceride lipase affects enzyme activity and lipid droplet binding. *J Biol Chem* 2008;283:17211–20.
- [47] Cornaciu I, Boeszoermenyi A, Lindermuth H, Nagy HM, Cerik IK, Ebner C, et al. The minimal domain of adipose triglyceride lipase (ATGL) ranges until leucine 254 and can be activated and inhibited by CGI-58 and G0S2, respectively. *PLoS One* 2011;6:e26349.
- [48] Kulminkaya N, Radler C, Viertlmayr R, Heier C, Hofer P, Colaco-Gaspar M, et al. Optimized expression and purification of adipose triglyceride lipase improved hydrolytic and transacylation activities in vitro. *J Biol Chem* 2021;297:101206.
- [49] Zeissig S, Dougan SK, Barral DC, Junker Y, Chen ZG, Kaser A, et al. Primary deficiency of microsomal triglyceride transfer protein in human abetalipoproteinemia is associated with loss of CD1 function. *J Clin Invest* 2010;120:2889–99.
- [50] Haemmerle G, Lass A, Zimmermann R, Gorkiewicz G, Meyer C, Rozman J, et al. Defective lipolysis and altered energy metabolism in mice lacking adipose triglyceride lipase. *Science* 2006;312:734–7.
- [51] Trites MJ, Clugston RD. The role of adipose triglyceride lipase in lipid and glucose homeostasis: lessons from transgenic mice. *Lipids Health Dis* 2019;18:204.
- [52] Ahmadian M, Duncan RE, Varady KA, Frasson D, Hellerstein MK, Birkenfeld AL, et al. Adipose overexpression of desnutrin promotes fatty acid use and attenuates diet-induced obesity. *Diabetes* 2009;58:855–66.
- [53] Hofer P, Taschler U, Schreiber R, Kotzbeck P, Schoiswohl G. The lipolysome—a highly complex and dynamic protein network orchestrating cytoplasmic triacylglycerol degradation. *Metabolites* 2020;10.
- [54] Kulminkaya N, Oberer M. Protein-protein interactions regulate the activity of adipose triglyceride lipase in intracellular lipolysis. *Biochimie* 2020;169:62–8.
- [55] Lundquist PK, Shivaiah KK, Espinoza-Corral R. Lipid droplets throughout the evolutionary tree. *Prog Lipid Res* 2020;78:101029.
- [56] Rava P, Hussain MM. Acquisition of triacylglycerol transfer activity by microsomal triglyceride transfer protein during evolution. *Biochemistry* 2007;46:12263–74.
- [57] Sellers JA, Hou L, Athar H, Hussain MM, Shelness GS. A drosophila microsomal triglyceride transfer protein homolog promotes the assembly and secretion of human apolipoprotein B - implications for human and insect lipid transport and metabolism. *J Biol Chem* 2003;278:20367–73.
- [58] Rava P, Ojakian GK, Shelness GS, Hussain MM. Phospholipid transfer activity of microsomal triacylglycerol transfer protein is sufficient for the assembly and secretion of apolipoprotein B lipoproteins. *J Biol Chem* 2006;281:11019–27.
- [59] Sakers A, De Siqueira MK, Seale P, Villanueva CJ. Adipose-tissue plasticity in health and disease. *Cell* 2022;185:419–46.